Precision targeting of autoreactive B cells in systemic lupus erythematosus using anti-9G4 idiotope synthetic immune receptor T cells

Jin Liu^{1,2,3,4}, Yuanxuan Xia^{1,2,3,5}, Brian J. Mog³, Colin Gliech^{1,2,3}, Elana Shaw^{1,2,3}, Dylan Ferris¹, Brock Moritz^{1,2,3}, Tolulope O. Awosika³, Sarah R. DiNapoli³, Stephanie Glavaris³, Kyle J. Kaeo^{1,2,3}, Xuyang Li³, Nikita Marcou³, Alexander H. Pearlman³, Taha S. Ahmedna³, Regina Bugrovsky⁶, Iñaki Sanz⁶, Chetan Bettegowda^{3,5}, Suman Paul^{3,7}, Victoria Duarte Alvarado^{8,9}, Denis Wirtz^{4,8,9,10}, Daniel Goldman¹, Michelle Petri¹, Kenneth W. Kinzler^{3,7}, Shibin Zhou^{3,7}, Felipe Andrade¹, Bert Vogelstein^{3,4,7}, and Maximilian F. Konig^{1,2,3,8,*}

Affiliations:

*Correspondence to:

Maximilian F. Konig, MD
Division of Rheumatology, Department of Medicine
The Johns Hopkins University School of Medicine
1550 Orleans Street
CRB2, Rm 516
Baltimore, MD 21287
Email: konig@jhmi.edu

¹Division of Rheumatology, Department of Medicine, The Johns Hopkins University School of Medicine, Baltimore, MD, USA

²Center for Autoimmunity and Immuno-Oncology, The Johns Hopkins University School of Medicine, Baltimore, MD, USA

³Ludwig Center for Cancer Genetics and Therapeutics, Howard Hughes Medical Institute, Sidney Kimmel Comprehensive Cancer Center, The Johns Hopkins University School of Medicine, Baltimore, MD, USA

⁴Department of Pathology, The Johns Hopkins University School of Medicine, Baltimore, MD, USA

⁵Department of Neurosurgery, The Johns Hopkins University School of Medicine, Baltimore, MD, USA

⁶Emory University School of Medicine, Atlanta, GA, USA

⁷Department of Oncology, The Johns Hopkins University School of Medicine, Baltimore, MD, USA

⁸Johns Hopkins Institute for Nanobiotechnology, The Johns Hopkins University, Baltimore, MD, USA

⁹Department of Chemical and Biomolecular Engineering, The Johns Hopkins University, Baltimore, MD, USA

¹⁰Department of Biomedical Engineering, The Johns Hopkins University, Baltimore, MD, USA

Competing Interests

M.F.K. is a consultant to Alexion Pharmaceuticals, Allogene, Amgen, Argenx, Atara Biotherapeutics, Bristol Myers Squibb, Legend Biotech, Mucommune, Revel Pharmaceuticals, Sana Biotechnology, and Sanofi. M.F.K. received research support from Blackbird Labs, NorthStar Medical Radioisotope, and TBD Pharmaceuticals, Inc. S.P. is a consultant to Merck and received payment from QVIA and Curio Science. M.F.K., S.P., B.V., K.W.K., and S.Z. are founders of, hold equity in, and are consultants to TBD Pharmaceuticals, Inc. C.B. is a consultant to TBD Pharmaceuticals, Inc. K.W.K. and B.V. are founders of Thrive Earlier Detection, an Exact Sciences Company. K.W.K. is a consultant to Thrive Earlier Detection. B.V., K.W.K., and S.Z. hold equity in Exact Sciences. B.V., K.W.K., and S.Z. are founders of or consultants to and own equity in Clasp, Neophore, and Personal Genome Diagnostics. B.V. and K.W.K. hold equity in Haystack Oncology and CAGE Pharma. B.V. is a consultant to and holds equity In Catalio Capital Management, S.Z. has a research agreement with BioMed Valley Discoveries. I.S. is a consultant to Bristol Myers Squibb (AcTION Steering Committee), Eli Lilly, GlaxoSmithKline, iCell Gene Therapeutics, Kyverna Therapeutics, and Novartis. C.B. is a consultant to Depuy-Synthes, Bionaut Labs, Haystack Oncology, Galectin Therapeutics, and is a co-founder of OrisDx and Belay Diagnostics. M.P. is a consultant to Autolus Therapeutics, Bristol Myers Squibb, Cabaletta Bio, Caribou Biosciences, iCell Gene Therapeutics, Kyverna Therapeutics, and Novartis. F.A. has received consulting fees and/or royalties from Celgene, Inova, Advise Connect Inspire, and Hillstar Bio, Inc. The companies named above, as well as other companies, have licensed technologies from The Johns Hopkins University. Licenses to these technologies are or will be associated with equity or royalty payments to the inventors as well as to Johns Hopkins University. The Johns Hopkins University has filed patent applications related to technologies described in this paper on which J.L., S.P., B.V., M.F.K. are listed as inventors. The terms of these arrangements are being managed by The Johns Hopkins University according to its conflict-of-interest policies.

Keywords: autoimmunity, systemic lupus erythematosus, immune effector cell therapy, chimeric antigen receptor, chimeric T cell receptor, 9G4 idiotope, VH4-34

Abstract

Chimeric antigen receptor (CAR)-T cell therapies that broadly target B cells can achieve complete remission in severe systemic lupus erythematosus (SLE) but carry an increased risk of infection and cytokine-related toxicities that limit their use. Alternative strategies that combine the potency of immune effector cell therapies with more precise targeting approaches have the potential to control disease without the challenges of broad immunosuppression. B cells expressing immunoglobulin heavy variable gene 4-34 (IGHV4-34)-derived B cell receptors (BCRs) are a major source of disease-relevant autoantibodies in lupus and other autoimmune diseases. Here, we exploit a common feature of IGHV4-34 BCRs, namely the 9G4 idiotope (9G4id), to develop precision cellular immunotherapies that target autoreactive B cells. Anti-9G4 CAR-T cells and anti-9G4 chimeric T cell receptor (cTCR) T cells, integrating anti-9G4 antibody fragments into a re-engineered TCR scaffold, eliminated autoreactive Ramos B cells expressing SLE patient-derived 9G4id BCRs with equal potency, while sparing non-9G4 Ramos B cells. Using SLE patient PBMCs, autologous anti-9G4 cTCR-T cells and anti-9G4 CAR-T cells selectively depleted primary human 9G4id B cells, while maintaining total B cell numbers. Similarly, anti-9G4 T cells eliminated B cells expressing 9G4id BCRs from patients with cold agglutinin disease and Burkitt lymphoma. Compared to broad targeting with CD19 CAR-T cells, anti-9G4 T cell therapies showed lower cytokine release (~6-8-fold for interferon [IFN]-y). In addition, anti-9G4 cTCR-T cells showed ~17-fold lower IFN-y secretion compared to anti-9G4 CAR-T cells, despite achieving similar cytotoxicity. Together, our findings suggest that anti-9G4 precision cellular therapies provide a strategy to selectively target pathogenic B cells in SLE, while minimizing risks of infection and cytokine-related toxicities.

Introduction

Systemic lupus erythematosus (SLE) is a potentially life-threatening multisystem autoimmune disease that predominantly affects women of childbearing age¹. Despite significant therapeutic advances, achieving disease remission in SLE remains challenging², and uncontrolled disease activity often results in irreversible end-organ damage¹. Currently available drugs are broadly immunosuppressive and have narrow therapeutic indices, leading to infections – a major cause of mortality in SLE – and other dose-limiting toxicities³. Therapies that control disease without impairing protective immune responses are critically needed, yet such therapies remain elusive.

Antinuclear antibodies are a canonical feature of SLE⁴, mediate tissue damage⁵, and can precede the onset of clinical symptoms by years⁶. As sources of pathogenic autoantibodies, targeting B cells and plasma cells has been a major therapeutic focus⁷. The use of monoclonal antibodies targeting CD20+ B cells has shown limited efficacy in SLE8-11, achieving only incomplete depletion of B cells in lymphoid organs and autoimmune target tissues^{12, 13}. By contrast, recent successes in repurposing more potent therapeutic modalities targeting B cells, including bispecific T cell engagers and chimeric antigen receptor (CAR)-T cells, have confirmed the transformative potential of B cell-directed therapies for the treatment of lupus¹⁴⁻²¹. Autologous CD19 CAR-T-cells, which can effectively deplete B cells in relevant tissue niches¹³, can achieve normalization of most autoantibody levels and complete - and in some cases durable disease remission in patients with severe lupus^{16, 17}. Nonetheless, excess morbidity and mortality from infection and cytokine-related toxicities observed with current immune effector cell therapies – including cytokine release syndrome (CRS)²², immune effector cell-associated neurotoxicity syndrome (ICANS)²³, and delayed neutropenia¹⁷, currently limit broad use, particularly for patients with non-refractory lupus or preclinical disease. These considerations motivate precision immunotherapies that selectively eliminate autoreactive B cells while preserving protective immunity, thereby reducing the risk of infection. To date, such efforts have largely been focused on autoimmune diseases that are organ-specific or driven by a single protein antigen²⁴, leveraging the fact that autoreactive B cells, though diverse, are distinguished from normal B cells by surface expression of BCRs that bind self-antigen²⁵. This can be exploited by antigenspecific therapies that target these BCRs directly through their cognate autoantigen²⁶⁻³⁰.

Antigen-specific strategies are attractive but are challenged in SLE by the extensive repertoire of autoantigens (>180) targeted by autoreactive B cells and their secreted autoantibodies³¹, including nucleic acids (e.g., dsDNA)³¹⁻³³, proteins (e.g., histones, DNAse1L3, Sm, U1-ribonucleoprotein, Ro52, Ro60)³⁴⁻³⁶, lipids (e.g., cardiolipin)^{34, 37}, and carbohydrates (e.g., I/i blood group antigens)³⁸. This diversity dramatically limits the feasibility of antigen-specific therapies in SLE and necessitates alternative strategies. One orthogonal approach is to target autoreactive BCRs independently of their antigen-binding regions through unifying structural elements, such as the shared use of immunoglobulin variable heavy (VH) chains. For instance, the B cell compartment in SLE is uniquely characterized by a marked expansion of autoreactive B cell clones that use VH4-34 in their BCRs, irreversibly selected during V-D-J recombination in early B-cell development³⁹. The framework region 1 (FR1) of VH4-34 encodes the 9G4 idiotope (9G4id), a

germline-encoded, conformational epitope that directly binds self-antigens (e.g., "i" and "I" blood group antigens and the glycoprotein CD45/B220)38, 40. 9G4id B cells are therefore inherently autoreactive and normally restrained by peripheral tolerance checkpoints. In healthy individuals, they are excluded from germinal centers, and affinity-matured 9G4id B cells are therefore underrepresented in the memory B-cell compartment. However, in SLE, 9G4id B cells are licensed to participate in germinal center reactions, generating IgG+ memory B cell and plasma cells³⁹. These 9G4id B cells are sources of many autoantibodies in SLE^{34, 41, 42}, including antinuclear, anti-dsDNA, anti-histone, anti-DNAse1L3, anti-Sm/RNP, anti-Ro52, anti-Ro60, and anti-cardiolipin antibodies (through binding of their affinity-matured complementarity determining regions [CDRs]), in addition to their reactivity to red blood cell and immune cell antigens (through the germline-encoded FR1). 9G4 antibodies are specific for SLE (sensitivity 45-70%; specificity >95%) and correlate with disease activity^{43, 44}. Notably, SLE patients treated with belimumab, a BAFFinhibiting monoclonal antibody, show a significant loss of VH4-34+ plasmablasts⁴⁵. Additionally, lupus disease flares following peripheral B cell depletion with rituximab are characterized by rises in 9G4id antidsDNA antibodies⁴⁶. These data suggest that 9G4id B cells have a relatively rapid turnover after B celltargeted therapies. Given their central role in active lupus and general dispensability in health, 9G4id B cells are a promising target for the depletion of autoreactive B cells in SLE.

In this study, we describe several precision cellular therapies targeting 9G4id B cells for the treatment of SLE and other 9G4id B cell-associated diseases. Comparing synthetic immune receptor designs, we show that CRISPR-engineered anti-9G4 CAR-T and cTCR-T cells are highly potent and specific at eliminating 9G4id autoreactive B cell lines and primary B cells from SLE patients, while showing significantly lower cytokine release compared to pan-B cell-targeted CAR-T cells. We found that anti-9G4 cTCR-T cells, as compared to anti-9G4 CAR-T cells, further mitigated cytokine release despite similar cytotoxicity, suggesting that cTCR-based cellular therapies may have favorable safety profiles for the treatment of patients with autoimmune diseases.

Results

Anti-9G4 cTCR-T cells and CAR-T cells have similar capacity to bind the 9G4id

Pan-B cell-targeted cellular therapies that are currently being repurposed for the treatment of autoimmune diseases almost invariably use CARs as synthetic immune receptors. To design and comparatively test anti-9G4 CAR (hereafter "9G4-CAR") constructs for the selective targeting of 9G4id B cells, we grafted an anti-9G4 single-chain variable fragment (scFv), using the variable light (VL) chain-linker-variable heavy (VH) chain orientation, onto second-generation CAR scaffolds comprising different linker peptides (a flexible poly-glycine-serine $[G_4S]$ or a more rigid five amino acid "EAAAK" linker), hinge domains (CD8 α , IgG4, CD3 ζ , or $[G4S]_3$), transmembrane domains (CD28 or CD3 ζ), a CD28 costimulatory domain (all constructs), and a CD3 ζ signaling domain (all constructs). A total of six 9G4-CAR designs were tested with varying extracellular domain size, flexibility, and membrane anchoring to

optimize immune synapse formation and to accommodate the large size of the target antigen (BCR) and the membrane-distal epitope "QW (15) AVY" (Fig. 1A, Fig. S1A).

While CARs confer high cytotoxicity against cells that express target antigens at a high surface density (e.g., CD19), CAR-T cells have been shown to lack efficacy at low or even moderate surface antigen densities (<200-5000/cell)^{47, 48}. As B cells differentiate into plasma cells, alternative splicing skews immunoglobulin expression from membrane-bound to secreted forms, sharply reducing surface BCR density^{49, 50}; thus, precision cellular therapies that retain cytotoxicity at low or ultra-low antigen densities may be more effective for autoimmune diseases where pathogenic B cells are contained in the plasma cell compartment (i.e., diseases not appropriately treated by CD19-CAR-T cells). Different to CARs, TCR signaling is tuned for high sensitivity, enabling T cells to mount effective cytotoxic responses against targets presenting very low antigen densities such as mutant peptide-HLA complexes on cancer cells⁵¹. Interestingly, recent work has shown that re-engineered cTCRs⁵² in some designs termed STARs⁵³—retain TCR-like sensitivity, enabling robust killing at very low antigen densities (<10 molecules per cell)⁵⁴. These designs fuse antibody fragments to a truncated TCR scaffold, thereby combining CARlike binding with TCR-like signaling. To potentially extend the spectrum of targetable autoreactive B-cell lineage cells that can be targeted, we designed anti-9G4 T cells that use re-engineered chimeric TCRs (cTCRs) as synthetic immune receptors (Fig. 1A). For this, we grafted anti-9G4 antibody fragments to the N-terminus of the TCRα and/or TCRβ chains, with endogenous variable domains removed, using two orthogonal designs (Fig. 1A). In one design, 9G4-cTCR1, an anti-9G4 scFv is fused to a truncated TCRa chain via a rigid EAAAK linker, while the TCRβ variable domain (Vβ) chain is truncated without additions. In a second design, 9G4-cTCR2, the anti-9G4 scFv is split across the TCR: the VH domain is fused to truncated TCRα and the VL domain to truncated TCRβ, each joined by an EAAAK linker (Fig. 1A).

To compare synthetic immune receptors under matched genomic and transcriptional contexts, we leveraged CRISPR/Cas (Cas9 or Cas12a/Cpf1)-mediated homology-directed repair (HDR) to introduce all constructs into the first exon of the TCRα constant (*TRAC*) gene locus of primary human T cells, simultaneously abrogating expression of the endogenous TCRα chain (**Fig. 1B**)^{54, 55}. The TCRβ constant (*TRBC*) gene loci were concurrently knocked out to avoid mispairing and expression of the engineered T cells' endogenous TCRs, a potential source of alloreactivity during extended co-culture killing assays. In all designs, expression of the cTCR or CAR transgene was driven by the elongation factor-1 alpha (EF1α) promoter, and a truncated nerve growth factor receptor (tNGFR) was included as a reporter for edited cell identification and purification⁵⁴. Controls included *TRAC/TRBC* double-knockout T cells (TCR-KO) and unedited T cells. Edited T-cell purity following CRISPR/Cas editing was measured by flow cytometry quantifying tNGFR and CD3 epsilon (CD3ε) expression, as each TCRαβ heterodimer associates with two CD3ε subunits (and CD3ε surface expression is lost after *TRAC/TRBC* KO without successful cTCR knockin)⁵⁶. Using this approach, initial editing efficiencies of approximately 15% were increased to 86-93% following positive selection (**Fig. 1C, Fig. S1B-C**).

Overall, tNGFR was expressed at comparable surface densities in all engineered anti-9G4 T cells (Fig. 1D-E, Fig. S1D-E), confirming successful editing of TRAC. CAR designs showed comparable surface tNGFR expression to one another (Fig. S1D-E), and a modestly higher expression than in cTCR designs (P<0.0001; Fig. 1D-E), potentially due to the smaller CAR constructs size. As expected, 9G4-CARs and TCR-KO T cells did not show CD3 ϵ surface expression due to the disruption of TCR α and TCR β constant chains, which precludes surface trafficking of CD3 ϵ (Fig. S1D-E). In contrast, 9G4-cTCR constructs (cTCR1, cTCR2) showed only 2-fold lower surface CD3 ϵ expression than unedited T cells (P<0.0001; Fig. 1D-E), with no difference between cTCR1- and cTCR2-T cells (P=ns; Fig. 1D-E).

To directly compare the expression and functional availability of the relevant antibody fragments in all synthetic immune receptors, we further stained engineered anti-9G4 T cells with established monoclonal 9G4id (clones 627A11, 75G12, 88F7)³⁴. Despite comparable tNGFR expression across CAR designs, anti-9G4 CAR EAAAK-CD8α-Hinge showed higher binding capacity to 9G4id than other CARs (*P*<0.001; Fig. S1D-F), and higher binding to 9G4id compared to 9G4-cTCR constructs (*P*<0.05). cTCR2-T cells bound slightly more to monoclonal 9G4id than cTCR1-T cells (*P*<0.01; Fig. 1D-F). Interestingly, clone 75G12 stained TCR-KO T cells and unedited T cells independent of anti-9G4 synthetic immune receptor expression (Fig. 1D, Fig. S1D), mirroring its reported ability to bind other immune cells⁴². Together, these results confirmed the successful engineering 9G4-targeted synthetic immune receptors in primary human T cells and reveal design-specific differences in receptor display and binding.

9G4-CAR-T cells and cTCR-T cells selectively kill SLE-9G4id B cell lines with comparable potency

To functionally test the potency and specificity of our cellular therapies, we generated model B cell lines by replacing the native BCR of Ramos B cells, a human Burkitt lymphoma cell line, with monoclonal BCRs of interest. This was achieved by editing *IGH* locus of Ramos B cells using CRISPR/Cas9 HDR to express a single-chain BCR/antibody construct containing a heavy chain constant region splice junction⁵⁷. This strategy simultaneously disrupts the endogenous BCR while allowing for expression of both membrane-bound (BCR) and secreted forms (antibody) of the transgenic monoclonal immunoglobulin under the control of endogenous regulatory elements. All BCR/antibody constructs were designed as a single-chain molecule linking the desired light chains and variable heavy chains with a Strep-tag II-containing linker peptide, allowing for detection and positive selection of surface-expressed BCRs (**Fig. 2A-B**). Using this approach, we generated autoreactive B cell lines expressing one of three SLE patient-derived 9G4id monoclonal BCR/antibodies (SLE 9G4id BCR_{627A11}, BCR_{75G12}, and BCR_{88F7}, respectively) and a control B cell line expressing a non-9G4id (VH4-4+) monoclonal BCR/antibody (BCR_{VH4-4}) (**Fig. 2C**).

Surface expression of 9G4id BCRs on autoreactive Ramos B cells (SLE 9G4id BCR_{627A11}, BCR_{75G12}, and BCR_{88F7}) and absence of 9G4id BCRs on non-9G4 control Ramos B cells (BCR_{VH4-4}) were confirmed by flow cytometry using a monoclonal anti-9G4 antibody (**Fig. 2C**). Finally, we determined the surface expression levels of 9G4id BCRs on engineered 9G4id Ramos B cells and primary human 9G4id B cells

isolated from human PBMCs by flow cytometric staining. BCR densities on engineered 9G4id B cells mirrored the surface expression levels on primary human 9G4id B cells (*P*=ns; Fig. 2D).

Having established a B cell model, we next compared the potency and specificity of our engineered immune effector in co-culture with SLE 9G4id Ramos B cell lines (BCR_{672A11}, BCR_{75G12}, and BCR_{88F7}) and control non-9G4 Ramos B cells (BCR_{VH4-4}). First, we tested the cytotoxicity of engineered T cells expressing five different 9G4 CAR designs against SLE 9G4id BCR_{627A11} Ramos B cells. Compared to TCR-KO control T cells, which did not deplete target or control B cells, all designs of 9G4 CAR-T cells showed complete elimination of SLE 9G4id BCR_{627A11} B cells, while preserving non-9G4 BCR_{VH4-4} Ramos B cells (control vs CAR-T, P<0.0001 for all effector-to-target cell (E:T) ratios) (**Fig. S1G**). Differences in cytotoxicity between the tested 9G4 CAR-T cell designs were not observed at higher E:T ratio (E:T=10:1, 5:1, 2.5:1, P=ns) (**Fig. S1G**). At lower E:T ratios (i.e., 1.25:1 and 0.62:1), 9G4 CAR EAAAK-CD8 α and 9G4 CAR (EAAAK) $_3$ showed the highest cytotoxicity (CAR EAAAK-CD8 α and CAR (EAAAK) $_3$ vs other CARs, P=0.045; CAR EAAAK-CD8 α vs CAR (EAAAK) $_3$ P=ns) (**Fig. S1G**). Given its surface expression (**Fig. S1D-F**), 9G4 CAR T cells with EAAAK-CD8 α Hinge (hereafter "9G4-CAR-T cells") were prioritized to investigate the potency of 9G4-CAR-T cells in comparison to 9G4-cTCR1- and cTCR2-T cells.

We next directly compared the potency and specificity of 9G4 cTCR1-T cells, 9G4 cTCR2-T cells, and 9G4 CAR-T cells using the Ramos B cell model. For this, we performed cytotoxicity assays in which we co-cultured 9G4 cTCR- and 9G4 CAR-T cells with one of three SLE 9G4id Ramos B cell lines (BCR672A11, BCR_{75G12}, or BCR_{88F7}) or non-9G4 Ramos B cells (BCR_{VH4-4}). After four days of co-culture, we quantified the absolute number of live, single Ramos B cells (GFP+) by flow cytometric staining of StrepTag II in edited BCRs (Fig. 3A). Compared to control T cells, co-culture with 9G4 CAR-T cells, 9G4 cTCR1-T cells, and cTCR2-T cells led to a marked reduction in 9G4id Ramos B cells (control vs CAR-T, cTCR1, and cTCR2, at all E:T ratios, respectively, P<0.05) (Fig. 3B), while non-9G4 Ramos B cells were not depleted. In addition, cytotoxicity observed with 9G4 CAR-T cells was not significantly different from 9G4 cTCR1-T cells or 9G4 cTCR2-T cells (Fig. 3B). Next, we compared the cytotoxicity of the different precision cellular therapies by live-cell imaging, longitudinally quantifying Ramos B cells by their expression of green fluorescent protein (GFP) (Fig. 3C). In a four-day co-culture of our synthetic immune receptor T cells with one of three SLE 9G4id Ramos B cell lines and control non-9G4 Ramos B cells, 9G4 CAR-T cells, 9G4 cTCR1-T cells, and 9G4 cTCR2-T cells all controlled target 9G4id Ramos cell growth (all anti-9G4 T cells vs. control T cells; P<0.0001) (Fig. 3D-G, Video 1), as determined by measuring green integrated intensity over time. In contrast, non-9G4 Ramos B cells (irrelevant B cells) were not impacted by co-culture with anti-9G4 T cells (P=ns) (Fig. 3C, 3H, Video 2). These results also showed no significant differences in cytotoxicity between 9G4 CAR-T cells and 9G4 cTCR-T cells (P=ns) (Fig. 3D). Repeated stimulation assays (RSAs) can showcase early T cell exhaustion and were shown to be good predictors of in-vivo efficacy⁵⁴. We therefore extended our model by administering additional B cells every 3 days to a 12-day co-culture of engineered anti-9G4 T cells and Ramos B cells. As before, we observed that 9G4 CAR-T cells, 9G4 cTCR1-T cells, and 9G4 cTCR2-T cells maintained robust and comparable potency against SLE 9G4id Ramos B cells with repeated challenge, without impairing non-9G4 B cells (**Fig. S2A-D**). Interestingly, when cocultured with cTCR-T cells, we observed outgrowth predominantly of BCR_{75G12}-negative B cells (**cTCR1/cTCR2 vs CAR, P<0.01; Fig. S2B-D**), suggesting antigen escape which is not expected when targeting primary B cells in patients with autoimmune disease. In contrast, coculture with 9G4 CAR-T cells resulted in markedly reduced expansion of BCR_{75G12}-negative populations (CAR vs control T cells, P<0.001) (**Fig. S2B**) as well as non-9G4 B cells (CAR vs control/cTCR1/cTCR2, P<0.05) (**Fig. S2C**), suggesting these are off-target effects mediated by 9G4 CAR-T cells.

We next aimed to investigate whether engineered anti-9G4 T cells can abrogate 9G4id autoantibody production. To this end, we measured 9G4id antibody levels and anti-dsDNA antibody levels in the co-culture supernatants by ELISA. Compared to control T cells, we observed a consistent reduction in both 9G4id and anti-dsDNA antibody production after co-culture with engineered anti-9G4 T cells (control vs CAR-T, cTCR1, and cTCR2, respectively, *P*<0.0001) (Fig. 3I-J). Supernatants of SLE 9G4id BCR_{75G12} (clone 75G12) showed 9G4id antibodies but no reactivity to dsDNA (Fig. 3J), consistent with previous findings³⁴. These results demonstrate the potency of 9G4 synthetic immune receptor T cells, while also suggesting a negligible effect of 9G4id autoantibodies secreted by Ramos B cells on the cytotoxicity of engineered T cells.

Engineered anti-9G4 T cells deplete 9G4id B cells in cold agglutinin disease and clonal B cell disorders

We next investigated whether engineered anti-9G4 T cells show similar efficacy against 9G4id B cells that drive other disease states. Cold agglutinins (CAs) are cold-activated antibodies that bind to red blood cells at low temperature, resulting in their agglutination and autoimmune hemolytic anemia^{58, 59}. In patients with cold agglutinin disease (CAD), a clonal B-cell lymphoproliferative disorder, IgM CAs are almost exclusively encoded by the VH4-34 gene and specific for I/i antigens expressed on red blood cells (bound by the 9G4id)⁶⁰⁻⁶⁴. To confirm whether engineered anti-9G4 T cells could eliminate B cells driving CAD, we generated three 9G4id Ramos B cell lines expressing different CAD patient-derived, CA+ BCRs (CAD 9G4id BCR_{KAU}, BCR_{FS-2}, and BCR_{FS-1}, respectively). Surface expression levels of the 9G4id BCRs was confirmed using monoclonal anti-9G4 antibody by flow cytometry (**Fig. S3A**). To evaluate the specificity and cytotoxicity of 9G4 CAR-T cells and 9G4 cTCR1-T cells against CAD 9G4id B cells, we co-cultured CAD 9G4id Ramos B cells with engineered anti-9G4 T cells or control T cells (**Fig. S3B**). All CAD 9G4id B cell clones were eliminated by both 9G4 CAR-T cells and 9G4 cTCR1-T cells (no engineered T cells vs other E:T ratios, *P*<0.01) (**Fig. S3C-D**), while non-9G4 BCR_{VH4-4} cells were preserved. Interferon (IFN)-γ secretion by anti-9G4 synthetic immune receptor T cells was detected only in the presence of target cells, as quantified in co-culture supernatants by ELISA (**Fig. S3E**).

We have recently highlighted the potential for 9G4id targeting in other disease states, including B cell cancers of the central nervous system where suitable patients may be readily identified by BCR

repertoire sequencing of cerebrospinal fluid (CSF) cells⁶⁵. An overrepresentation of the 9G4id has been reported across a multitude of B cell cancers⁶⁶⁻⁷⁰. The consistent presence of 9G4id suggests that its ability of binding self-antigens critically supports malignant B cell survival. To confirm that our engineered anti-9G4 T cells show potency also against endogenous 9G4id BCRs expressed by B cell cancers, we took advantage of the fact that wild-type Ramos RA1 B cells, a Burkitt lymphoma cell line, naturally use VH4-34⁷¹. After confirming surface expression of endogenous 9G4id BCR (**Fig. S3F**), we co-incubated 9G4 CAR-T cells and 9G4 cTCR1-T with wild-type Ramos B cells, which expectedly resulted in efficient elimination of 9G4id B cell clones (no engineered T cells [E:T 0:1] vs other E:T ratios, *P*<0.05) (**Fig. S3G-H**). IFN-γ was secreted by engineered anti-9G4 T cells only in the presence of target cells and in a dosedependent manner (**Fig. S3I**). Together, these data show that precision cellular therapies targeting the 9G4id can selectively eliminate 9G4id BCR B cells across disease states (autoimmune disease, lymphoproliferative disorder, B cell cancer), with comparable potency, and despite various somatic mutations accrued by their BCRs during affinity maturation. Antibodies secreted by 9G4id Ramos B cells, engineered or wild-type, did not preclude cytotoxic killing of target cells by anti-9G4 T cells.

9G4-targeted cTCR-T cells demonstrate favorable cytokine release characteristics for the treatment of autoimmune diseases

Cytokine-related toxicities, including CRS and ICANS, are known and potentially life-threatening complication of immune effector cell therapy, commonly observed in patients with cancer^{22,23}. While these toxicities tend to be less severe in patients with autoimmune diseases, cytokine-related toxicities remain a major barrier. Strategies that can reduce these risks may allow cellular therapies to be applied to patients with less severe disease and in settings that require less intense monitoring. To understand how the use of different synthetic immune receptors may modulate the risk of cytokine-related toxicities, we quantified cytokine release and T cell activation in in-vitro co-cultures. Overall, cytokine secretion did not correlate with improve cytotoxicity in our study. 9G4 CAR-T cells, when co-cultured with 9G4id B cells, secreted significantly higher levels of cytokines compared to 9G4 cTCR1- or 9G4 cTCR2-T cells (Fig. S3E, S3I; Fig. 4A-B; Fig. S4A-I), despite comparable effectiveness in killing target B cells. Specifically, 9G4 cTCR1-T cells and 9G4 cTCR2-T cells compared to 9G4-CAR-T cells released significantly lower levels of IFN-γ (cTCR1 and cTCR2 vs CAR-T, in co-incubation with all 9G4id B cells, *P*<0.01) (Fig. 4A), Granzyme A and B (CAR-T vs cTCR1 and cTCR2, coincubation with 9G4id BCR_{627A11} cells, *P*<0.0001), IL-2Rα (*P*<0.0001), IL-4 (*P*<0.001), IL-6 (*P*<0.0001), IL-8 (*P*<0.0001), TNF-α (*P*<0.0001), TNF-β (*P*<0.0001), GM-CSF (*P*<0.0001) (Fig. 4B), suggesting a potential advantage in reducing the risk of CRS.

The increased cytokine release by 9G4 CAR-T cells was mirrored by increased T-cell proliferation following antigen-exposure by co-culture with 9G4id B cells (CAR-T vs cTCR1 and cTCR2, coincubation with all 9G4id B cells, P<0.0001) (**Fig 4C-D**). Notably, proliferation of T cells independent of 9G4id B cells was observed for 9G4-CAR-T cells but did not occur in 9G4-cTCR-T cells (CAR-T vs cTCR-T, coincubation with all 9G4id B cells, P<0.0001) (**Fig 4C-D**). Our results demonstrate that both 9G4CAR-T cells and 9G4

cTCR-T cells can completely and efficiently eliminate 9G4id B cells. 9G4 cTCR-T cells showed mitigated cytokine release compared to CAR-T cells, which may be preferable for the treatment of patients with autoimmune diseases which may not rely on the persistence of engineered T cells for optimal outcomes and dictate a lower tolerance for severe adverse events.

Engineered anti-9G4 T cells selectively deplete autoreactive B cells from patients with SLE

Having comprehensively evaluated our cellular therapies in isogenic B cell lines, we next set out to test the potency and specify of anti-9G4 T cells against primary human B cells isolated from patients with SLE. For this, we chose four SLE patients from a convenience sample (**Table S1**). The 9G4id peripheral blood B-cell frequencies in SLE patient PBMCs were determined by flow cytometric staining with anti-CD19 and anti-9G4 antibodies. Total B cells comprised 7.31% (patient 1), 5.99% (patient 2), 5.3% (patient 3), and 3.78% (patient 4) of total PBMCs. 9G4id B cells comprised 6.3% (patient 1), 5% (patient 2), 5% (patient 3), and 6.11% (patient 4) of total B cells (**Table S2**). Co-cultures were conducted using PBMCs and donor-matched T cells to eliminate alloreactivity. For this, primary human T cells were isolated from PBMCs of selected SLE patients, activated, and engineered to generate autologous 9G4 CAR-T cells, 9G4 cTCR1-T cells, and second-generation CD19 CAR-T cells, utilizing the same strategy described above (editing rate, purity after enrichment, and T-cell functional properties are summarized in **Table S2**).

Engineered or unedited T cells were then co-cultured with matched patient PBMCs. After a 6-day co-culture in B-cell stimulation media, cells were transferred to FluoroSpot plates and incubated in the same media for another 24 hours to further promote B cell differentiation into antibody-secreting cells (ASCs). Subsequently, the number of 9G4id IgG ASCs and total IgG ASCs were quantified using the FluoroSpot assay (Fig. 5A). Incubation with 9G4 CAR-T cells and 9G4 cTCR-T cells resulted in 95-100% reduction in the number of IgG+ 9G4id ASCs (control T cells vs 9G4-CAR-T cells and cTCR-T cells, P<0.0001) (Fig. 5B), without reduction of total IgG+ ASCs (control T cells vs 9G4-CAR-T cells and cTCR-T cells, P=ns) (Fig. S5A). Autologous CD19 CAR-T cells, by contrast, depleted 100% of IgG+ ASCs compared to autologous anti-9G4 T cells and control T cells (P<0.0001) (Fig. S5A). We further confirmed these FluoroSpot results by bulk mRNA BCR repertoire sequencing (Fig. 5C-D, Fig. S5F-G, Data Files S1-S9). After co-culture of PBMCs with either 9G4 CAR-T cells or 9G4 cTCR-T cells, over 99.7% of the 9G4id B-cell compartment was depleted (control T cells vs 9G4-CAR-T cells and cTCR-T cells, P < 0.05) (Fig. 5D), while other B cell compartments were not depleted (P>0.05 for various IHGV genes). We observed that B cells using IGHV2-26, IGHV6-1 and IGH4-30-2 genes expanded after co-incubation, but no other compartment was depleted. To further validate these findings, we cocultured 9G4 CAR-T or 9G4 cTCR-T cells with primary B cells from healthy donors. Flow cytometric staining with anti-9G4 antibody, which detects all isotypes (IgG, IgA, IgM) of 9G4id B cells (Fig. S5B), confirmed selective depletion of 9G4id B cells (control T cells vs 9G4 CAR-T cells and cTCR-T cells, P<0.05) (Fig. S5D), while preserving the overall B-cell compartment (control T cells vs 9G4 CAR-T cells and cTCR-T cells, P=ns) (Fig. S5C). Interestingly, at lower E:T ratios (0.3:1 and 0.6:1), 9G4 CAR-T cells demonstrated approximately two-fold greater cytotoxicity than 9G4 cTCR1-T cells (P<0.05) **(Fig. S5D)**, but secreted significantly higher levels of IFN- γ (1315 pg/mL vs. undetectable in cTCR1-T cells, P<0.0001 at E:T = 0.6:1) **(Fig. S5E)**. Consistently, these results suggest that 9G4-cTCR-T cells achieve comparable cytotoxic efficacy at relevant E:T ratios while exhibiting markedly mitigated cytokine release relative to CAR-T cells.

Finally, to understand fundamental differences to currently available CD19 CAR-T cells, we interrogated cytokine secretion at 48 hours of co-incubation of engineered or control T cells with SLE patient PBMCs. Compared to autologous CD19 CAR-T cells, both 9G4 CAR-T cells and 9G4 cTCR1-T cells produced markedly lower levels of effector cytokines, including IFN-y (CAR: 6-fold lower, P=0.004; cTCR1: 8-fold lower, P=0.003) (Fig. 5E), IL2Ra (CAR: 2-fold lower, P=0.042; cTCR1: 2-fold lower, P=0.025) (Fig. **5E)**, Granzyme A (CAR: 7-fold lower, P=0.037; cTCR1: 5-fold lower, P=0.056) (Fig. 5E), Granzyme B (CAR: 2-fold lower, P=0.087; cTCR1: 2-fold lower, P=0.079) (Fig. 5E). Additionally, CD19 CAR-T cells produced significantly higher amount of pro-inflammatory cytokines such as TNF-β (CAR: 4-fold lower, P<0.0001; cTCR1: 4-fold lower, P<0.0001) (Fig. 5E) and GM-CSF (CAR: 7-fold lower, P=0.038; cTCR1: 15-fold lower, P=0.024) (Fig 5E), which are commonly associated with CRS ⁷². Compared to conventional CD19 CAR-T cells that target B cells indiscriminately and require close monitoring for CRS in clinical use, 9G4 cTCR-T and 9G4 CAR-T cells that target a much smaller B-cell population exhibited markedly attenuated cytokine release, suggesting a potentially safer approach. This combination of specificity and reduced cytokine production has the potential to meaningfully mitigate the risk of severe adverse events while preserving cytotoxic efficacy. Together, our findings highlight the feasibility of precision cellular therapies directed against 9G4id B cells for the treatment of SLE and other autoimmune diseases. Importantly, such targeted strategies may provide a safer alternative to pan-B cell-directed CAR-T therapies, particularly in patients with mild or moderate diseases, by minimizing both cytokine-related toxicities and the risk of infection.

Discussion

Cellular therapies that indiscriminately target B cells can achieve drug-free disease remission in patients with severe autoimmune diseases, but the risk of serious adverse events, including infection and cytokine-related toxicities⁷³, precludes their widespread use. Precision cellular therapies engineered to selectively target pathogenic B cell subsets are therefore being explored to harness the potency of immune effector cell therapies without compromising protective immunity³⁰. If successful, such approaches could move immune effector cells from salvage care to safer, frontline interventions that transform treatment across the spectrum of autoimmune disease.

One such approach comprises antigen-specific cellular immunotherapies that are engineered to target autoreactive B cells directly through binding of their cognate autoantigen²⁶⁻²⁹. These strategies, however, are only suitable for the treatment of autoimmune diseases in which one autoantigen is the primary target of the pathogenic B cell response. In SLE, a systemic autoimmune disease where CAR-T cell therapy can achieve sustained remission¹⁴⁻¹⁶, the broad autoreactome targeted by disease-relevant B cells makes antigen-specific approaches unfeasible³¹.

To overcome this, we developed a precision cellular therapy for the treatment of SLE that targets the 9G4 idiotope present in VH4-34+ BCRs, exploiting a shared origin and structural feature of autoreactive B cells in SLE^{41, 42}, including those cross-reactive with dsDNA, DNAse1L3, Sm/RNP, Ro52, and cardiolipin^{3441, 42}. To this end, we evaluated the efficacy and specificity of T cells expressing different synthetic immune receptor formats, including CARs and cTCRs, for the targeting autoreactive 9G4id B cells. We found that all engineered anti-9G4 T cells showed high specificity and eliminated 9G4id B cells without depleting non-9G4 B cells. This was observed regardless of somatic hypermutation, reactivity, or disease origin (i.e., SLE, CAD, or lymphoma) of the targeted B cells. Notably, 9G4id B cells, whether engineered B cell lines or primary B cells from patients with SLE, were eliminated despite their ability to secrete autoantibodies, supporting that the presence of soluble autoantibodies does not meaningfully impair targeting BCR-specific B cells with different strategies, as recently demonstrated in pemphigus vulgaris²⁴. Deep, selective depletion of autoreactive B cell subsets, as compared to the broad targeting of B cells, represents a major step towards immune effector cell therapies that do not increase the risk of infection.

Future work will focus on adapting these synthetic immune receptors in ways that obviate conditioning therapy, which by itself causes transient immunosuppression⁷⁴. While the need of conditioning therapy for the treatment of autoimmune diseases is being investigated for ex-vivo engineered cellular therapies⁷⁵, in-vivo delivery of CAR or cTCR mRNA/DNA to T cells represents an emerging opportunity to advance precision cellular therapies without immunosuppression⁷⁶⁻⁷⁹. These approaches allow for the direct generation of engineered T cells within the patient, thereby eliminating the need for complex ex-vivo manipulation and precluding conditioning. In patients with SLE, transient expression of synthetic immune receptors in T cells may be sufficient to ameliorate or control disease without risk of

long-term immune system alterations or secondary malignancy⁷⁹⁻⁸¹. Leveraging in-vivo delivery of mRNA to introduce anti-9G4 synthetic immune receptors may ultimately present a sufficient, safe, and more scalable option for patients with mild to moderate lupus, in whom potential adverse events of conditioning therapy (e.g., infection, infertility) and currently unquantifiable long-term risks of gene editing (e.g., secondary cancers) represent barriers to treatment with current engineered cellular therapies^{80, 82, 83}.

Cytokine-related toxicities, including CRS, ICANS, and delayed cytopenia^{17, 23}, are another major barrier to administering T cell therapies at scale, necessitating close monitoring and early therapeutic intervention. While these toxicities appear to be less severe in patients with autoimmune diseases than in B cell cancers⁸⁴, CRS remains common^{15-17, 85, 86} and high-grade neurotoxicity has been reported^{87, 88}. Minimizing cytokine release is therefore essential to improve the safety of cellular therapies, enable their use in outpatient settings, and extend their application to patients with non-life-threatening autoimmune disease. One opportunity to mitigate the risk of cytokine-related toxicities is to reduce the target cell burden, a benefit of all precision cellular therapies that target only a fraction of total B cells (e.g., 0.1-10%)^{89,} 90. This theoretical benefit was observed in our study where direct comparison of matched-donor anti-9G4 T cells and CD19 CAR-T cells against SLE patient PBMCs showed significantly reduced cytokine release with targeting only 9G4id B cells (~5-6.3 % of total B cells). Cytokine release may also be curtailed through strategic selection of effector cell types and phenotypes, as well as through optimization of immune receptor architecture and signaling components⁹¹. In studying different synthetic immune receptor formats in direct comparison, we found that 9G4 CAR-T cells demonstrated the highest release of IFN-y, while cytokine release was markedly reduced when using cTCR-T cell formats. These differences may be explained by the co-stimulatory domain (i.e., CD28) in the CAR constructs, in addition to fundamental differences in receptor regulation and immune synapse formation between CARs and TCRs^{48, 54, 92-97}. 9G4 CAR-T cells exhibited antigen-independent expansion, consistent with constitutive signaling, which was importantly not observed in 9G4 cTCR-T cells. The differences in cytokine release between both immune receptor scaffolds was more pronounced when targeting 9G4id Ramos B cells, derived from transformed B cells of a patient with Burkitt lymphoma, but attenuated in co-cultures with SLE patient PBMCs. This may reflect several factors, including differences in target cells (e.g., resistance to cytotoxic killing pathways in transformed vs. primary B cells), differences in the functional state of effector T cells in SLE patients vs. healthy donors⁹⁸, or a combination thereof. While co-stimulatory domains are essential for durable responses in cancer, the need for long-term T cell persistence for durable remission in autoimmune disease is unproven, and persistence beyond deep B cell depletion (conceptually referred to as "immune reset" in the current literature) may in fact be detrimental. The reduced cytokine release by 9G4 cTCR-T cells in this study may suggest a favorable safety profile in patients with mild-to-moderate lupus or other autoimmune diseases, in whom engineered T cell persistence is not a goal.

Disease heterogeneity is a significant barrier to therapeutic interventions in lupus⁹⁹. While 9G4id B cells are a major source of pathogenic autoantibodies in lupus^{34, 41, 42}, it is unknown whether their deep

depletion alone suffices to ameliorate disease in all patients. The contribution of 9G4id B cells to organ damage likely varies among individuals, highlighting the need for diagnostics to identify patient subsets most likely to respond to precision immunotherapies. Such diagnostics may include BCR repertoire sequencing (to quantify VH4-34 clonal expansion)^{65, 100}, flow cytometry to enumerate class-switched 9G4id memory B cells³⁹, or immunoassays measuring levels of 9G4id autoantibodies longitudinally³⁴. Notably, autoreactive B cell clones outside the VH4-34 repertoire may contribute to disease. For instance, 9G4id antibody depletion in serum reduced anti-DNASE1L3 autoantibodies by up to 80% in SLE patients³⁴. However, we observed that 9G4id B cell depletion in SLE PBMCs fully eliminated anti-dsDNA B cells in some patients. Thus, it is conceivable that precision therapies targeting 9G4id B cells may control disease in some patients, while others may only achieve partial responses. Future research focused on comprehensively defining the contribution of 9G4id B cells in heterogenous disease cohorts of SLE will be critical to advance precision medicines for lupus.

The utility of 9G4-targeted therapies extends beyond SLE and could be of immense value in other B cell-driven diseases. One notable condition is cold agglutinin disease (CAD), a type of autoimmune hemolytic anemia where IgM autoantibodies bind to red blood cells at low temperatures, leading to their destruction¹⁰¹. These IgM autoantibodies are almost invariably encoded by the VH4-34 gene, making 9G4id B cells a promising target for therapeutic intervention^{63,64}. We and others have identified clonally expanded 9G4id B cells in the CSF of patients with multiple sclerosis (MS)⁶⁵, and similar contributions to autoantibody compartments are found in other autoimmune diseases¹⁰², an opportunity for their precision targeting in select patients guided by molecular diagnostics. Finally, 9G4-targeted immunotherapies may be promising precision therapeutics in patients with various B cells cancers which are abnormally enriched in VH4-34 usage⁶⁸. We expect that the selection and utility of different synthetic immune receptor designs will be dictated by the patient population, and benefits observed for the treatment of cancer may not be equally applicable for the patients with autoimmune diseases.

Figures

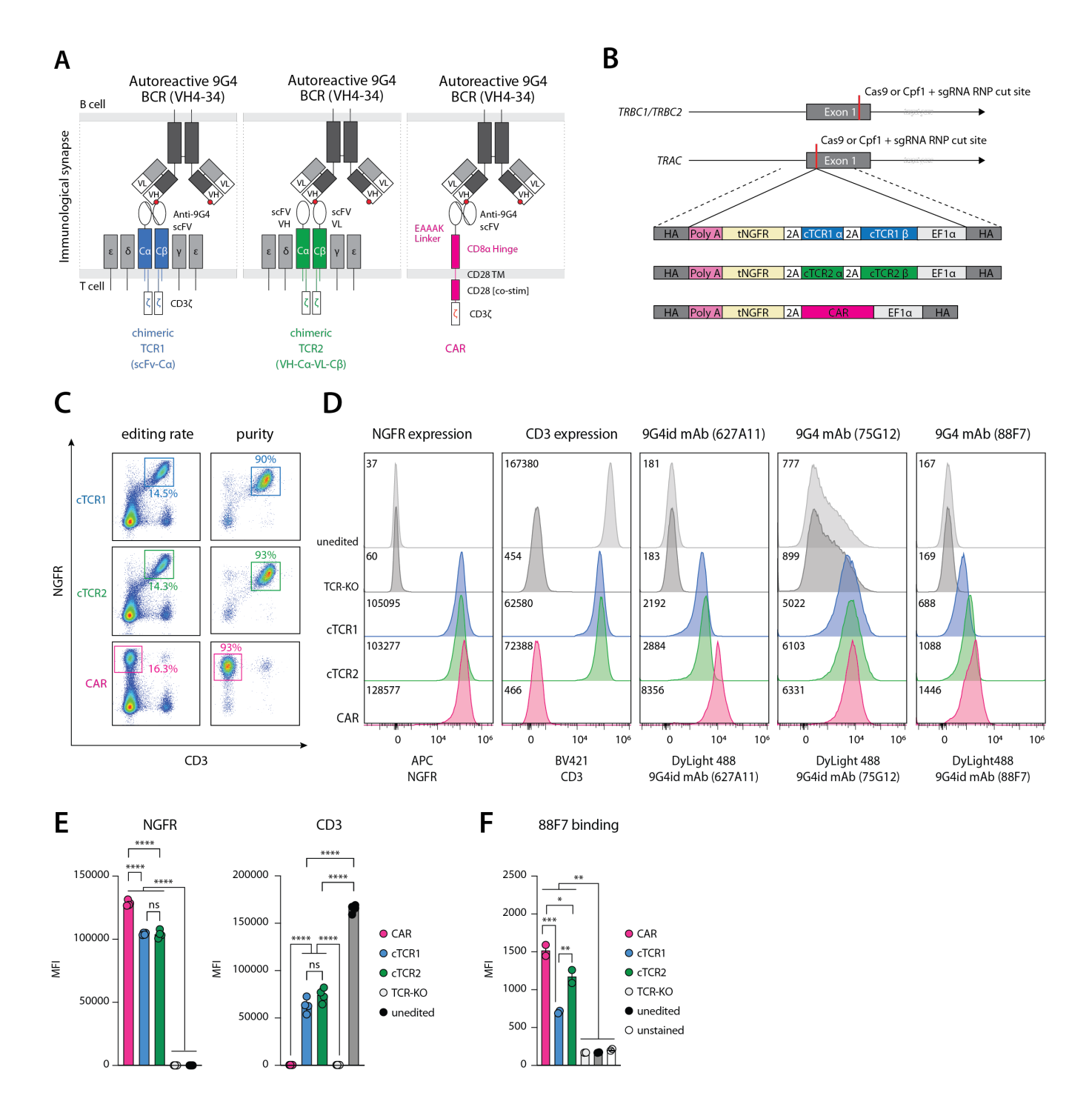


Figure 1. Expression of synthetic immune receptor in 9G4 CAR-T cells and 9G4 cTCR-T cells. (A) Diagrams of 9G4 cTCR1-, 9G4 cTCR2-T, and 9G4 CAR-T cells targeting 9G4id (VH4-34+) BCRs. The two cTCR constructs tested (cTCR1, cTCR2) are shown. cTCR1 comprises an anti-9G4 single-chain variable fragment (scFv) linked to a truncated TCR constant α (Cα) domain and a truncated TCR constant β (Cβ) domain, with the endogenous TCR variable domains removed. In comparison, cTCR2 comprises a split antibody fragment format that the immunoglobulin heavy (VH) chain of the anti-9G4 scFv to Cα and the immunoglobulin light (VL) chain to C\u03c3. TCR chains are similarly truncated to remove the endogenous TCR variable domains. The prioritized 9G4 CAR construct comprises an anti-9G4 scFv, an EAAAK linker, a CD8a hinge, a CD28 transmembrane (TM) domain, an intracellular CD28 co-stimulatory domain (co-stim), and an intracellular CD3 ζ signaling domain. ϵ , δ , γ , and ζ denote CD3 ϵ , δ , γ and ζ subunits/domains, respectively. The autoreactive BCR containing the 9G4 idiotope (pink dot) is shown for comparison. (B) Visual summary of the CRISPR/Cas HDR strategy used to simultaneous knock out TRBC1 and TRBC2 (KO). and knock-in synthetic immune receptor coding sequences into TRAC (KI). cTCR1, cTCR2, and CAR homology directed repair templates (HDRTs) are shown specifically. Double-stranded DNA (dsDNA) HDRTs used comprise an EF1a promoter (EF1a) sequence, Kozak sequence, signal peptide sequence, the synthetic receptor domain(s), a tNGFR sequence (for selection), Stop codon, and a simian virus 40 polyadenylation (poly A) sequence. Different proteins are separated by furin-2A (2A) sequences for expression. Homology arms (HAs) for the target locus are approximately 300 base pairs (bps) in length, flanking the above sequences. (C) Flow cytometric validation of editing rates of engineered T cells four days after nucleofection (left column) and purity after positive bead selection (right column). Edited cells were visualized by staining for tNGFR (CAR, cTCR1, cTCR2 expected to be positive) and/or CD3 epsilon (cTCR1, cTCR2 expected to be positive). Percentage of edited single, live T cells is shown before and after positive selection. (D) Histograms (from left to right) of flow cytometric staining for tNGFR, CD3 epsilon (CD3), and three monoclonal 9G4id derived from SLE patients (clones 627A11, 75G12, and 88F7). Median Fluorescence Intensity (MFI) for each staining is shown in each panel. (E) Statistical summary of MFIs observed for tNGFR and CD3 for 9G4 CAR-T, 9G4 cTCR1-T, 9G4 cTCR2-T cells, TCR knock-out (KO)-T cells (control), and unedited T cells (control). Data are shown as mean ± SD of 4 replicates. (F) Statistical summary of MFIs observed for binding of monoclonal 9G4id 88F7 in the same set of T cells. Data are shown as mean \pm SD of 2 replicates. ****P<0.0001, ***P<0.001, **P<0.01, *P<0.05, P=ns (not significant) by one-way ANOVA with Tukey's multiple comparison test. All statistical analyses are provided in the Supplementary Dataset.

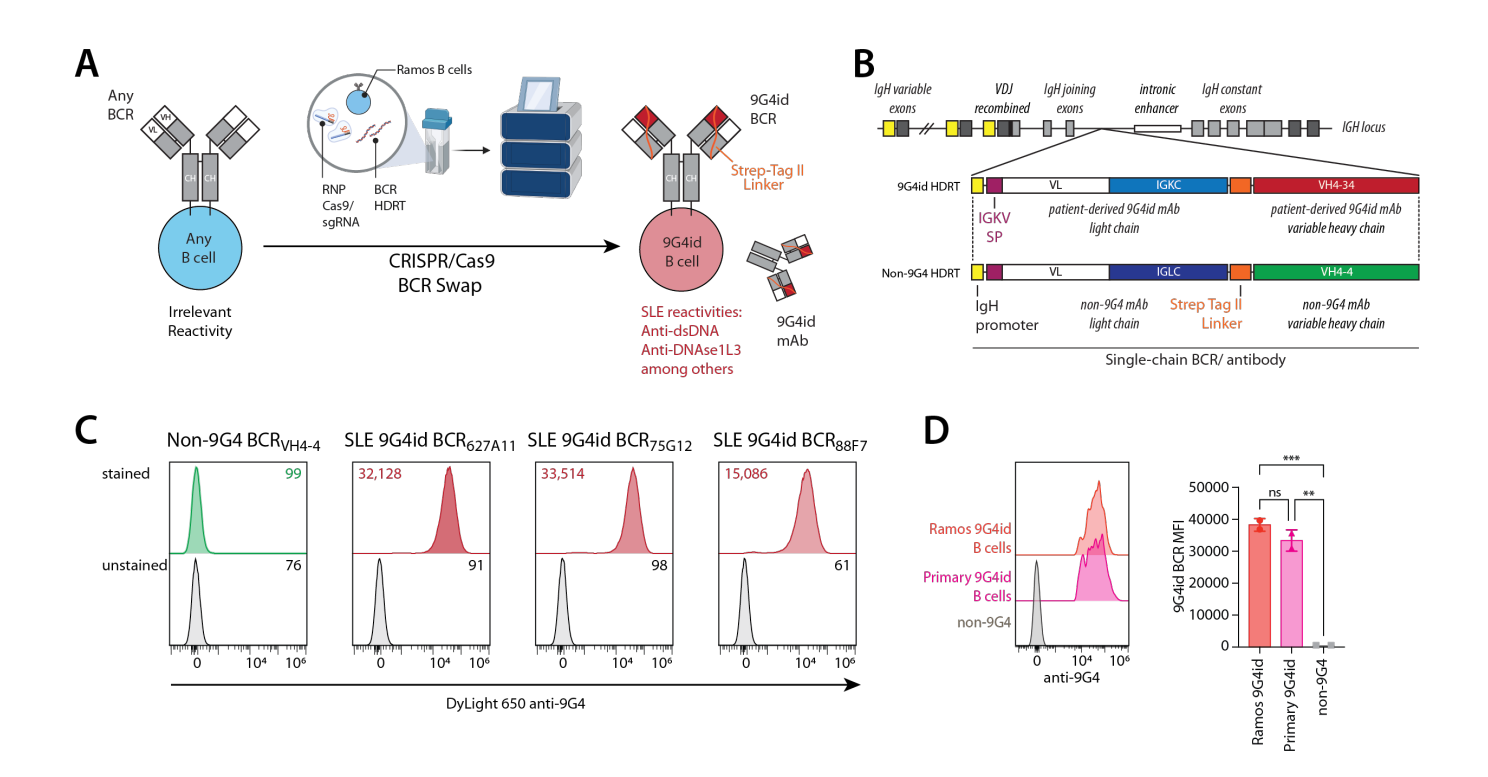


Figure 2. Generation of autoreactive Ramos B cell lines expressing SLE patient-derived, 9G4id BCRs/ antibodies. (A) Schematic of the experimental strategy to replace the endogenous BCR/antibody of Ramos B cells with desired patient-derived autoreactive BCR/ secreted antibody using CRISPR/Cas9mediated HDR. This strategy was employed to generate three Ramos B cell lines expressing autoreactive 9G4id (VH4-34+) BCRs from patients with SLE and one control BCR (VH4-4+). CRISPR, Clustered Regularly Interspaced Short Palindromic Repeats; RNP, ribonucleoprotein; sgRNA, single-guide RNA; HDRT, homology-directed repair template; dsDNA, double-stranded DNA. (B) Visual summary of the CRISPR/Cas9 HDR gene editing strategy used to introduce the paired immunoglobulin variable light (VL) and variable heavy (VH) chains of monoclonal BCR/antibody into the IGH gene locus, abrogating expression of the endogenous BCR. Monoclonal immunoglobulin of interest is expressed as a single-chain construct, incorporating a Strep-tag II linker used for detection and positive selection. (C) Flow cytometric staining of engineered Ramos B cell clones (non-9G4 [VH4-4] B cell clone, left panel; 9G4id SLE B cell clones, right panels) with an anti-9G4 antibody, after magnetic bead enrichment and single clone selection. Median Fluorescence Intensity (MFI) of each stained and unstained B cell clone is shown. (D) Comparison of 9G4id BCR expression levels on engineered SLE 9G4id Ramos BCR627A11 cells and primary human B cells by flow cytometric staining with an anti-9G4 antibody. Non-9G4 B cells are shown as a negative control. Data are shown as means ± SD of two technical replicates. Data are representative of n = 2 independent experiments. ***P<0.001, **P<0.01, P=ns (not significant) by one-way ANOVA with Tukey's multiple comparison test. All statistical analyses are provided in the Supplementary Dataset.

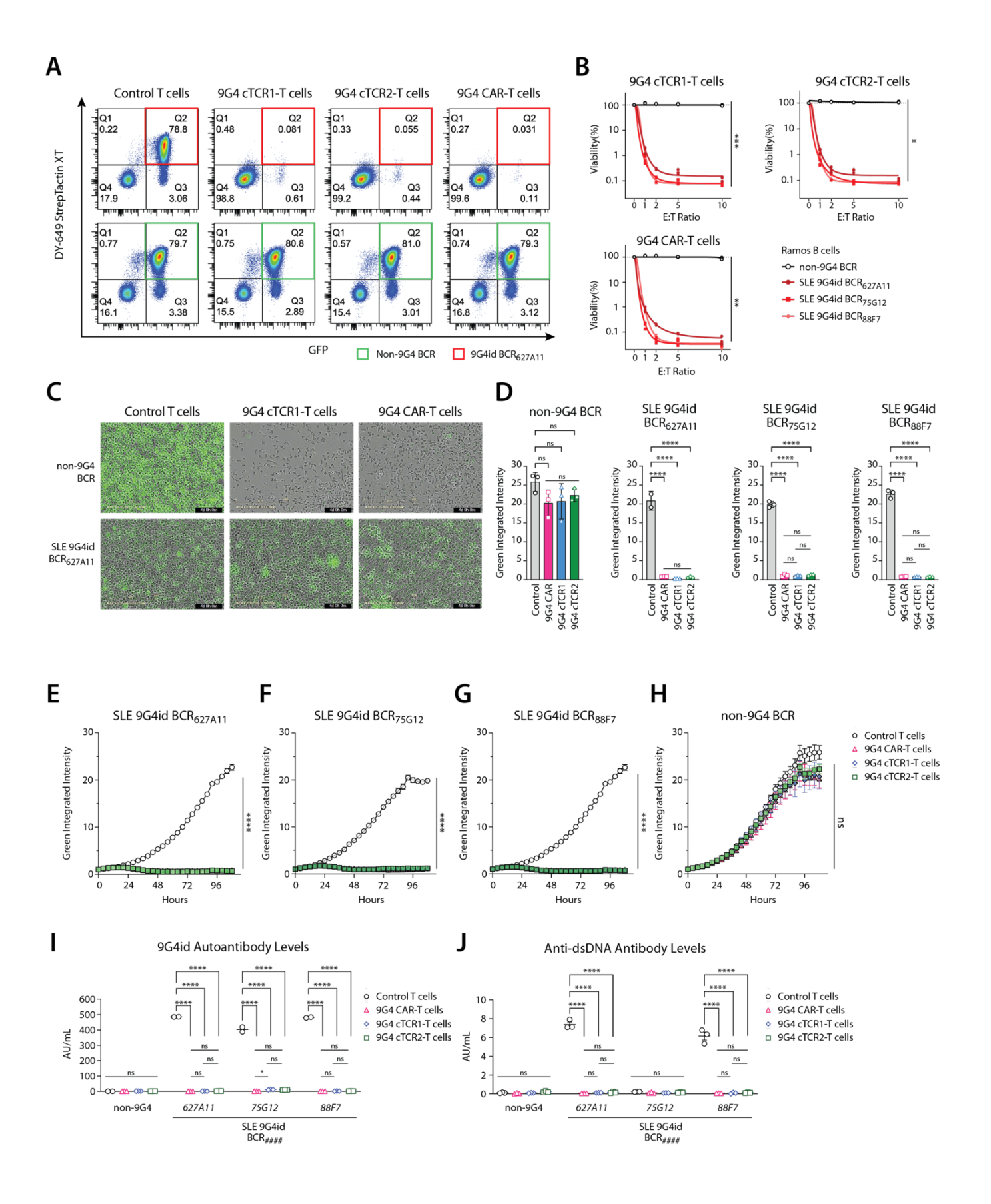


Figure 3. T cells engineered to express anti-9G4 synthetic immune receptors eliminate 9G4id B cells with comparable specificity and potency. (A) Representative flow cytometry plots illustrating selective killing of Ramos B cells expressing the SLE patient-derived, autoreactive 9G4id BCR_{627A11} (top row) at the end of co-culture with either control T cells, 9G4 cTCR1-T cells, 9G4 cTCR2-T cells, or 9G4 CAR-T cells (top panels, from left to right). 9G4id BCR_{627A11} B cells (Q2, top row), known to react with lupus antigens dsDNA, DNAse1L3, and cardiolipin, were eliminated by 9G4 cTCR1-T cells, 9G4 cTCR2-T cells, and 9G4 CAR-T cells, but not control T cells. Ramos B cells expressing a non-9G4 BCR/antibody (VH4-4), used as an irrelevant B cell control, were not depleted under the same conditions (Q2, bottom row). In this example, flow cytometric analysis of single, live cells after 4 days of co-incubation at an effector-to-target cell [E:T] ratio of 10:1 (100,000 edited T cells, 10,000 GFP+ Ramos B cells) is shown. B cells are identified as GFP+, DY649 StrepTactin XT+ cells (binding Strep-tag II in surface-expressed BCRs, Q2). T cells are visualized in Q4 as GFP-, StrepTactin XT- cells. (B) Percent viability of Ramos B cells (SLE 9G4id Ramos BCR_{627A11}, SLE 9G4id Ramos BCR_{75G12}, SLE 9G4id Ramos BCR_{88F7}, or non-9G4 BCR) at the end of coculture with either 9G4 cTCR1-T cells (top left graph), 9G4 cTCR2-T cells (top right graph), or 9G4 CAR-T cells (bottom left graph) for different E:T ratios (E:T=10:1, 100,000 edited T cells; E:T=5:1, 50,000 edited T cells; E:T=2.5:1, 25,000 edited T cells; E:T=1.25:1, 12,500 edited T cells; 10,000 B cells). The absolute numbers of single, live GFP+, StrepTactin XT+ B cells, as determined by flow cytometry, were used to calculate % viability. All data were normalized to the co-culture condition with control T cell (E:T=0). ***P<0.001, **P<0.01, *P<0.05; two-way ANOVA with Dunnett's multiple comparison test. (C-H) Coculture of GFP+ Ramos B cells (non-9G4 BCR, BCR_{627A11}, BCR_{75G12}, or BCR_{88F7}) with engineered anti-9G4 T cells (9G4 CAR, 9G4 cTCR1, or 9G4 cTCR2) or control T cells longitudinally analyzed by live-cell imaging for 108 hours (Incucyte SX5, 10x). (C) Representative images showing GFP+ Ramos B cells (non-9G4 BCR, top row; or 9G4id BCR_{627A11}, bottom row) in co-culture with control T cells (left panels), 9G4 cTCR1-T cells (middle panels), or 9G4 CAR-T cells (right panels) at 4 days (10x, phase contrast and green channel). (D) Ouantification of Green Integrated Intensity of GFP+ Ramos B cells (panels from left to right: non-9G4 BCR, BCR_{627A11}, BCR_{75G12}, or BCR_{88F7}) in co-culture with T cells (control T cells [Control], 9G4 CAR, 9G4 cTCR1, or 9G4 cTCR2). All data were normalized to day 0 of co-culture at same condition. ****P<0.0001, ns, not significant; one-way ANOVA with Tukey's multiple comparison test. (E-H) Changes in Green Integrated Intensity in co-cultures of with GFP+ Ramos BCR_{627A11} (E), BCR_{75G12} (F), BCR_{88F7} (G), or non-9G4 BCR B cells (H), as quantified by live-cell imaging. (I) Quantification of secreted 9G4id antibody levels by ELISA in culture supernatants of non-9G4 BCR Ramos B cells, BCR_{627A11} Ramos B cells, BCR_{75G12} Ramos B cells, or BCR_{88F7} Ramos B cells incubated with control T cells or engineered anti-9G4 T cells (9G4 CAR, 9G4 cTCR1, or 9G4 cTCR2). Comparisons are representative of n=2 experiments. (J) Quantification of secreted anti-dsDNA autoantibody levels by ELISA in the same co-culture supernatants. Comparisons are representative of n=2 experiments. Data are shown as mean ± SD of technical replicates. ****P<0.0001, *P<0.05, ns, not significant; two-way ANOVA with Tukey's multiple comparison test. All statistical analyses are provided in the Supplementary Dataset.

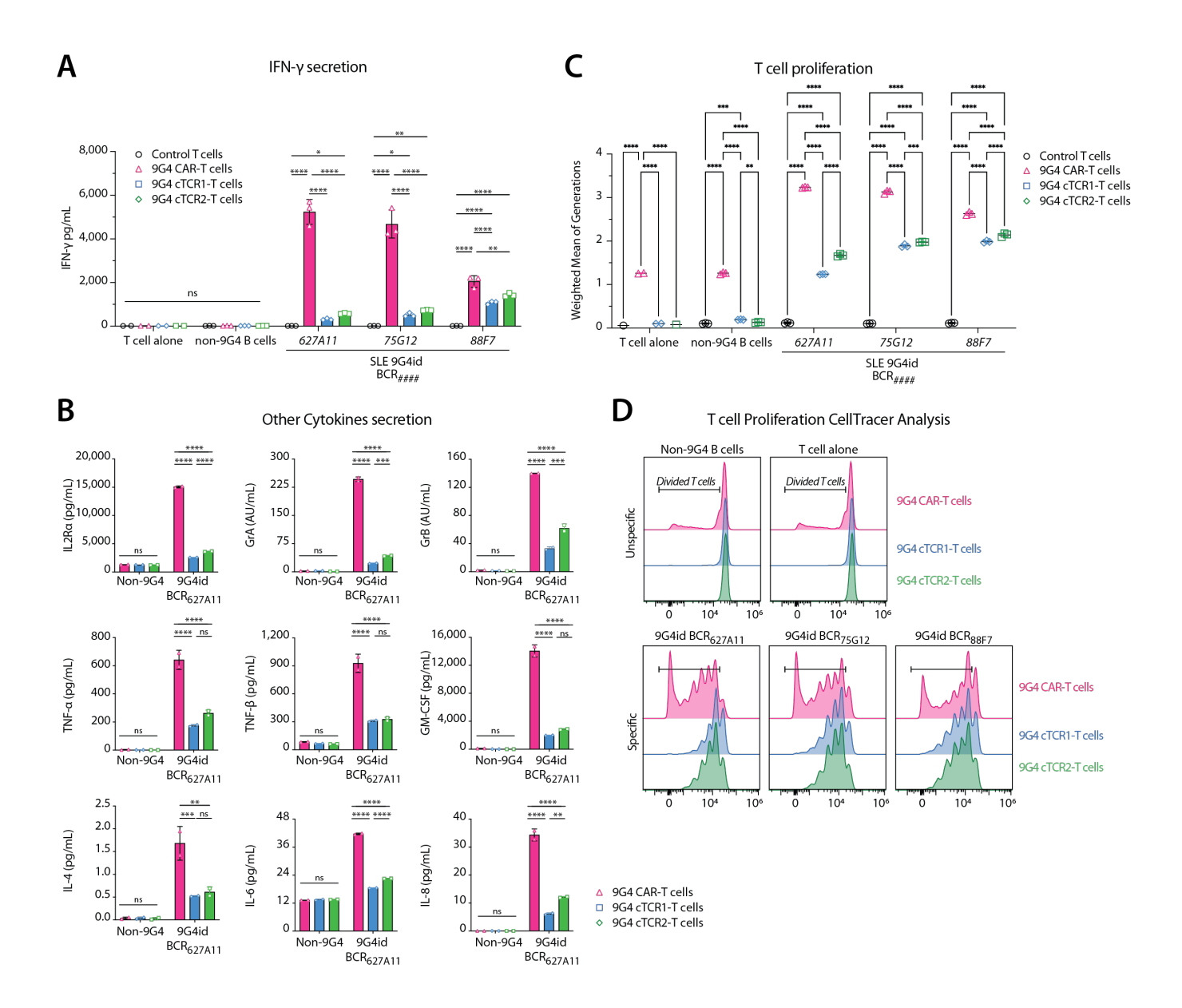


Figure 4. 9G4 cTCR-T cells restrain cytokine release and prevent antigen-independent expansion.

(A) To allow for direct comparison, different 9G4 synthetic immune receptor T cells (9G4 CAR-T cells, 9G4 cTCR1-T cells, 9G4 cTCR2-T cells) or control T cells were cultured with the SLE 9G4id Ramos BCR_{627A11}, BCR_{75G12}, BCR_{88F7}, or non-9G4 B cells (E:T=5:1, 62 hours). Quantification of IFN- γ in conditioned co-culture supernatants by ELISA is shown. Columns and error bars represent mean \pm SD. (B) Quantification of other cytokines (IL2Ra, TNF-a, TNF- β , GM-CSF, IL-4, IL-6, IL-8) and secreted cytotoxic granule proteins (granzyme A [GrA], granzyme B [GrB]) in co-culture supernatants of the same experiment shown in A (U-PLEX assay, Meso Scale). Columns and error bars show mean \pm SD. (C) Proliferation of T cells (9G4 CAR-T cells, 9G4 cTCR1-T cells, 9G4 cTCR2-T cells, or control T cells) in response to target B cells (SLE 9G4id Ramos BCR_{627A11}, BCR_{75G12}, BCR_{88F7}) or irrelevant B cells (non-9G4 BCR Ramos B cells) as determined by fluorescent dye dilution. Anti-9G4 synthetic immune receptor T cells and control T cells labeled with

CellTrace Violet (CTV) were cultured without B cells ("T cell only"), with non-9G4 BCR Ramos B cells, or with SLE 9G4id Ramos B cells (BCR_{627A11}, BCR_{75G12}, BCR_{88F7}) at an E:T ratio of 5:1. Flow cytometry was performed after 108 hours of co-incubation, and CTV dye dilution quantified in live, single T cells. Weighted average of generations (mean \pm SD) was calculated to quantify T-cell proliferation for statistical analysis. (D) Flow cytometric analysis of CTV dilution in single, live T cells, showing the percent of divided, engineered T cells (9G4 CAR, 9G4 cTCR1, or 9G4 cTCR2) in the presence of irrelevant B cells (non-9G4 B cells, top left panel), no B cells ("T cells only", top right panel), or SLE 9G4id Ramos B cell lines (bottom row panels). Comparisons are representative of n=2 independent experiments. ****P<0.0001, **P<0.005, ns=not significant; two-way ANOVA with Tukey's multiple comparison test.

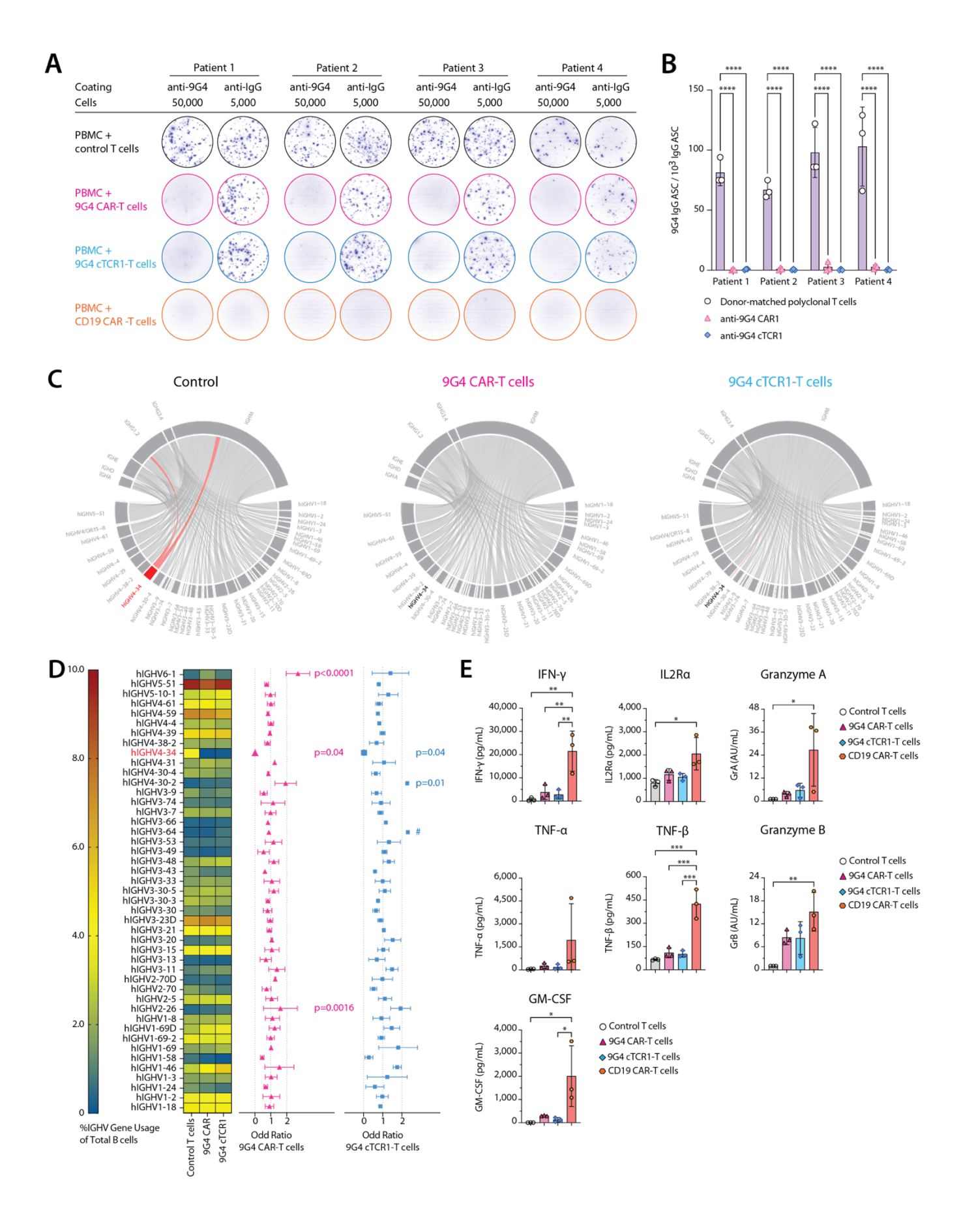


Figure 5. 9G4 CAR-T cells and 9G4 cTCR-T cells selectively eliminate 9G4id B cells in SLE patient PBMCs. (A) Results of B cell FluoroSpot assays showing selective killing of primary human 9G4id B cells/antibody secreting cells (ASCs) from patients with SLE in co-culture with autologous 9G4 CAR- or 9G4 cTCR-T cells. For this experiment, 100,000 PBMCs from SLE patients (n=4) were co-cultured with 5,000 9G4 donor-matched control T cells (autologous CD3+ T cells, no genetic modification), 9G4 CAR-T cells, 9G4 cTCR1-T cells, or CD19 CAR-T cells in B-cell stimulation/ differentiation media. After 6 days, cells were transferred to FluoroSpot 96-well plates coated with either anti-9G4 antibody (50,000 cells/ well) or anti-human IgG antibody (anti-hIgG, 5,000 cells/well). After 20 hours of incubation, spots corresponding to 9G4id+ ASCs or total hlgG+ ASCs were detected using fluorophore conjugated anti-hlgG antibody (shown in pseudocolor). (B) Quantification of results shown in A. The number of IgG 9G4id ASCs per 1,000 total IgG ASCs is shown. Autologous 9G4 CAR-T cells and 9G4 cTCR1-T cells both eliminated IgG 9G4id ASCs from patients with SLE. Two-way ANOVA with Tukey's multiple comparison test. (C) IGHV mRNA sequencing was performed at the end of co-culture of SLE PBMCs with either autologous control T cells (left), 9G4 CAR-T cells (middle), or 9G4 cTCR1-T cells (right). Chord diagrams of IGHV and IGHC gene usage show depletion of IGHV4-34+ B cell clonotypes which are predominantly found in the IgG1/2 and IgM compartment. Data show is for patient 3 as a presentative example. (D) Left, Heat map summarizing the usage of different IGHV genes (in % of total B cells) of B cells from SLE patients 1-3 after co-incubation with control T cells, 9G4 CAR-T cells, or 9G4 cTCR1-T cells, as determined by bulk repertoire sequencing. Right, forest plots depicting mean odds ratios and SD for IGHV gene usage in PBMCs (n=3) treated with donor-matched control T cells vs 9G4 CAR-T cells (pink tringles, left) or 9G4 cTCR1-T cells (blue squares, right), #denotes only one sample. One-way ANOVA with Dunnett's multiple comparison. (E) Quantification of cytokines (IFN-y, IL2Ra, TNF-a, TNF-B, GM-CSF) and secreted cytotoxic granule proteins (granzyme A [GrA], granzyme B [GrB]) in co-culture supernatants of SLE patient PBMCs (n=3) treated with 9G4 CAR-T cells, 9G4 cTCR1-T cells, conventional CD19 CAR-T cells, or control T cells at 48 hours (U-PLEX assay, Meso Scale). Data are shown as mean \pm SD. ****P< 0.0001, **P<0.001, **P<0.01, *P<0.05; one-way ANOVA with Tukey's multiple comparison.

Materials and Methods

Study Design

The goal of the study was to develop and evaluate synthetic immune receptor-T cell therapies for the precision targeting of 9G4id B cells in patients with lupus, aiming to eliminate pathogenic 9G4id B cells while sparing most normal B cell populations. Specifically, this study comparatively tested anti-9G4 CAR and anti-9G4 cTCR designs for the treatment of autoimmune diseases. Primary human T cells from healthy donors or patients with SLE were genetically modified using CRISPR-Cas12a to eliminate endogenous TCR expression and introduce anti-9G4 CAR or anti-9G4 cTCR constructs via homology-directed repair (HDR). Synthetic immune receptor expression in T cells was quantified by flow cytometry, and successfully edited T cells were enriched by positive selection. Ramos B cell lines were engineered using CRISPR-Cas9 HDR to replace endogenous BCR expression with patient-derived monoclonal BCRs from patients with SLE, cold agglutinin disease (CAD), or irrelevant BCRs, creating isogenic cell lines with and without 9G4id expression for specificity testing. T cell-mediated cytotoxicity was measured using live-cell imaging, flow cytometric enumeration of target cells, and (auto)antibody production. T cell activation was assessed by quantification of cytokine and chemokine secretion using enzyme-linked immunosorbent assay (ELISA) and Meso Scale U-PLEX. T-cell proliferation was interrogated through fluorescent dye dilution by flow cytometry. The function of engineered, donor-matched T cells to deplete primary 9G4id B cells from SLE patients was tested in PBMCs using both B cell FluoroSpot and bulk BCR repertoire sequencing. Comparative analyses between CAR-T and cTCR-T cell platforms were performed to evaluate potency, cytokine release, antigen-dependent and antigen-independent proliferation. Statistical tests, number of replicates, and number of experiments are listed in the figure legends.

Synthetic immune receptor design and generation

Nucleotide sequences encoding 9G4 cTCR, 9G4 CAR, and CD19 CAR constructs were designed in silico as described. Sequences were codon optimized for human expression, de-novo synthesized (GeneArt), and cloned into pUC19-derived vectors containing an EF1 α promoter, Kozak sequence, signal peptide, synthetic immune receptor domain(s), 2A ribosomal skip sequence, signal peptide, truncated nerve growth factor receptor (tNGFR), stop codon, and polyadenylate terminator, all flanked 5' and 3' by homology arms (HA) for the human *TRAC* locus. For cTCRs, fully human TCR α and TCR β chains separated by 2A sequences were linked to either anti-9G4 scFv via an EAAAK linker to TCR α (cTCR1), or by fusing VH and VL fragments of the anti-9G4 antibody to the TCR α and TCR β chains (cTCR2), respectively. CARs utilized second-generation CAR designs comprising a CD8 α signal peptide, various hinge domains, transmembrane domain, a CD28 co-stimulatory domain, and a CD3 ζ signaling domain. Homology-directed repair templates (HDRTs) for CRISPR editing were generated by PCR amplification from vector templates (Q5 Hot Start High-Fidelity 2X Master Mix, New England BioLabs), purified using AMPure XP Reagent (Beckman Coulter, A63880), eluted in nuclease-free water, and quantified using a NanoDrop spectrophotometer (Thermo Fisher).

Gene editing of primary human T cells

Peripheral blood mononuclear cells (PBMCs) were isolated from healthy donor leukopaks (STEMCELL) by Ficoll-Paque PLUS (Cytiva) gradient centrifugation and cryopreserved in CryoStor CS10 (BioLife Solutions). For some experiments, PBMCs were collected from patients with SLE under a Johns Hopkins Medicine IRB approved protocol (IRB00307779), cryopreserved in CryoStor CS10, and thawed for isolation and editing. CD3+ T cells were isolated from PBMCs by negative immunoselection (STEMCELL, 17951) and resuspended in RPMI-1640 (ATCC, 30-2001) supplemented with 10% FBS (Gibco, A5669701), 1% penicillin-streptomycin (P/S, Thermo Fisher, 15140163), 100 IU/mL recombinant human interleukin (IL)-2 (Proleukin, Prometheus Laboratories), and 5 ng/mL recombinant human IL-7 (BioLegend, 581908), hereafter called T-cell media. T cells were immediately activated with Dynabeads Human T-Activator CD3/CD28 (Thermo Fisher, 11132D) at a 1:1 bead-to-cell ratio for 48 hours, after which beads were removed with a magnet. To edit T cells, 50 pmols of Cas12a sgRNAs targeting either TRAC or TRBC were incubated with 25 pmols of Alt-R Cas12a (Cpf1) Ultra (IDT, 10001273) and Alt-R Cpf1 Electroporation Enhancer (IDT, 1076301) in Nuclease Free Duplex Buffer (IDT, 11-01-03-01) for 15 minutes to form RNPs, before combining both RNPs at a 1:1 volume ratio, TRAC- and TRBC-targeted RNPs were then incubated with 0.5 µg of cTCR/CAR HDRTs diluted in OptiMEM (Gibco). For each condition, 1x10⁶ T cells were pelleted at 90 x g for 10 minutes, resuspended in 20 µL P3 buffer (Lonza, V4XP-3032), and combined with 5 µL of Cpf1 RNP/HDRT complex. T cells were nucleofected in 16-well cuvettes (Lonza, V4XP-3032) using a 4D Nucleofector X-Unit (Lonza, AAF-1003X) and pulse code EH115. After nucleofection, 80 µL pre-warmed media without cytokines (RPMI-1640, 10% FBS, 1% P/S) was added to cells, and the cuvette strip was placed at 37°C, 5% CO₂ for 30 min. The recovered cells were then resuspended in T-cell media and incubated in 24-well plates at 37°C, 5% CO₂. Media was changed every 2-3 days, and T cells were expanded for at least 11 days until functional assays were performed. All sgRNA sequences are listed in the data supplement.

Generation of autoreactive human B cell lines

Ramos RA1 B cells (CRL-1596, ATCC) were cultured in RPMI-1640 (ATCC) supplemented with 10% FBS and 1% P/S, hereafter called Ramos media, in a humidified incubator at 37°C and 5% CO₂. Cells were transduced with IVISbrite Red F-luc-GFP (BD) lentiviral particles to enable the stable expression of green fluorescent protein (GFP) and firefly luciferase (Luc), and edited cells isolated by FACS using a BD FACSMelody Cell Sorter. To generate autoreactive 9G4id B cell lines, Ramos RA1 cells ("wild-type") were engineered using CRISPR/Cas9 homology-directed repair to express desired monoclonal BCRs and antibodies. Coding sequences of SLE patient-derived, autoreactive 9G4id BCRs (clones 627A11, 75G12, 88F7)³⁴, CAD patient-derived, autoreactive 9G4id BCRs (cold-agglutinin antibody clones KAU¹⁰³, FS-1 and FS-2^{104, 105}), and non-9G4 BCRs using VH4-4 were introduced into the *IGH* locus to replace the Ramos cell's endogenous BCR and to generate autoreactive Ramos B cells that express both soluble and membrane-bound immunoglobulin under control of a locus-specific promoter, while preserving natural splicing⁵⁷. Briefly, nucleotide sequences comprising IgVH promoter, signal peptide, immunoglobulin

variable light (VL), constant light (CL), Strep-tag II linker, and variable heavy (VH) chains, flanked by homology arms for the human *IGH* locus, were de-novo synthesized (GeneArt) and cloned into suitable vectors. HDRTs were generated as described above. To edit Ramos cells, 50 pmol of purified Cas9 nuclease (Alt-R SpCas9 Nuclease V3, IDT) was combined with 100 pmol of *IGH*-targeted Cas9 sgRNA (IDT, custom) and Alt-R Cas9 Electroporation Enhancer (IDT, 1075915) for 15 minutes at room temperature (RT). RNPs were then incubated with 60 pmol of HDRTs diluted in OptiMEM. For each condition, 1×10^6 Ramos cells were resuspended in 20 µL SF buffer (Lonza, PBC2-00675) and combined with 5 µL of Cas9 RNP/HDRT complex. Ramos cells were nucleofected in 16-well cuvettes using a 4D Nucleofector X-Unit and pulse code CV-104. After nucleofection, 80 µL pre-warmed Ramos media was added to cells, and the cuvette strip was placed at 37° C, 5% CO $_2$ for 30 min. The recovered cells were then resuspended in Ramos media and incubated in 24-well plates at 37° C, 5% CO $_2$. After one-week, edited cells were enriched by one or more rounds of positive selection using StrepTactin magnetic beads (iba, 2-5090-010). Edited cells were isolated by FACS based on robust GFP and engineered BCR expression, stained with DY649-StrepTactin XT (iba, 2-1568-050). Sorted cells were plated by limiting dilution to obtain individual autoreactive B cell clones. All sgRNA sequences are listed in the data supplement.

Flow cytometry

Flow cytometry was performed using an Attune NxT cytometer (Thermo Fisher). Cells of interest were labeled with a viability dye, either LIVE/DEAD Fixable Near-IR Dead Cell Stain (Thermo Fisher, L34975) or LIVE/DEAD Fixable Violet Dead Cell Stain (Thermo Fisher, L34955). T cells were stained with combinations of the following anti-human antibodies: APC anti-CD3 (clone SK7, BioLegend, 344812), Brilliant Violet (BV) 421 anti-CD3 (clone SK7, BioLegend, 344834), FITC anti-CD3 (clone SK7, BioLegend, 344804), APC anti-human CD271 (clone ME20.4, BioLegend, 345108), FITC anti-human CD271 (clone ME20.4, BioLegend, 345104), FITC anti-PD-1 (clone NAT105, BioLegend, 367412), APC anti-PD-1 (clone EH12.2H7, BioLegend, 329908), APC anti-CD8 (clone SK1, BioLegend, 344722), BV421 anti-CD8 (clone RPA-T8, BioLegend, 301036). The expression of cTCRs and CARs was assessed using DvLight 488conjugated (Abcam, ab201799) 9G4id IgG1 (clones 627A11, 75G12, 88F7), expressed in Expi293 cells (Gibco) and purified as described³⁴. When staining human PMBCs, Human TruStain FcX (BioLegend, 422302) was used. Ramos B cells were stained with combinations of the following anti-human antibodies: Alexa Fluor (AF) 488 anti-CD20 (clone 2H7, BioLegend, 302316), DyLight 650 anti-9G4 (conjugated in house; Abcam, ab201803), DY-649 Strep-Tactin XT (iba, 2-1568-050). Ramos cells were stained with AF488 anti-CD19 (clone SJ25C1, BioLegend, 363038), BV421 anti-CD19 (clone SJ25C1, BioLegend, 363018), AF488 anti-CD20 (clone 2H7, BioLegend, 302316), BV421 anti-CD20 (clone 2H7, BioLegend, 302330), DyLight 650 anti-9G4id. Flow cytometry data were analyzed with FlowJo v.10.1 software (BD).

In-vitro co-culture of engineered B cell lines

Anti-9G4 cTCR-T cells, CAR-T cells, or control T cells ("effector cells") were combined with 1x10⁴ autoreactive or unedited GFP+ Luc+ Ramos B cells ("target cells") at defined E:T ratios in T-cell media,

unless specified otherwise. Co-cultures were incubated for 2.5-4.5 days at 37°C, 5% CO₂, humidified air in tissue culture-treated 96-well microplates (Costar, Corning), as specified in the figure legends. Longitudinal killing of GFP+ Ramos Bcells was quantified every 4 hours using an Incucyte SX5, G/O/NIR module, and 10-20x objective (Sartorius). Green integrated intensity for each well normalized to day 0 was used for statistical analysis. Endpoint flow cytometry analysis of samples was conducted by gating on live, single GFP+ B cells. Viability was calculated by normalizing to the absolute B cell number in the control T cell groups using the formula number_{experimental well}/ number_{control well} x 100. At assay endpoint, conditioned co-culture media was also collected and stored for cytokine assays.

Repeated stimulation assays

In-vitro co-culture of human PBMCs

Cryopreserved PBMCs (1x10⁵ viable cells) collected from patients with SLE were thawed and combined with engineered, donor-matched human T cells (5x10³ viable cells) in serum-free media (ImmunoCult-XF B Cell Base Medium, supplemented with ImmunoCult-ACF Human B Cell Expansion Supplement, STEMCELL) or RPMI-1640 media (ATCC) supplemented with 10% FBS, 1% P/S, and human IL-2 and IL-7, as specified in figure legends. After 48 hours, conditioned co-culture media was collected and stored for cytokine assays, and new serum-free media was added. After another 48-96 hours of B cell activation, cells were collected and subjected to B cell FluoroSpot assay (Mabtech) and mRNA-based IgH repertoire sequencing (iR-RepSeq+, iRepertoire).

Autoantibody ELISAs

9G4id antibody levels were quantified in cell culture supernatants using an in-house ELISA. Briefly, polystyrene plates (Costar, 9018) were coated with 100 ng/well purified rat anti-9G4 antibody (IGM Biosciences) in PBS, pH 7.4, or PBS alone. Coated plates were washed with PBS 0.05% Tween-20 (PBS-T, Thermo Fisher) and remaining binding sites blocked with PBS-T containing 5% non-fat dry milk (PBS-TM) for 1 hour at RT. Culture supernatants were diluted 1:10 in PBS-TM 1%, added to washed plates, and incubated for 1 hour at RT, 150 rpm. Binding of human 9G4id antibodies was detected using HRP-conjugated goat anti-human IgM (Jackson ImmunoResearch, 109-035-129), diluted 1:2000 in PBS-TM 1%,

incubated for 1 hour at RT, 150 rpm, protected from light. TMB peroxidase substrate solution (SureBlue, KPL) was added to wells, and the reaction was stopped with $1M H_2SO_4$ (Thermo Fisher). Absorbance was measured at 450 nm (background 620 nm) using an Absorbance 96 microplate reader (Byonoy). Antibody levels were calculated in reference to wells coated with a serial dilution of native human IgM (Abcam, ab91117) that served as a standard. Anti-dsDNA antibodies in cell culture supernatants (1:5 diluted) were measured using a modification of the QUANTA Lite dsDNA ELISA (Inova, 708510), replacing the secondary antibody with HRP-conjugated goat anti-human IgM at 1:10,000 dilution.

FluoroSpot assay

9G4id antibody-secreting B cells in PBMCs from patients with SLE were measured using a modified B cell FluoroSpot assay. FluoroSpot plates (MabTech, X-05R-10) were coated with 1500 ng/well of rat anti-9G4 antibody or 1500 ng/well anti-human IgG (MT91/145, MabTech, 3850-3) in PBS pH 7.4 (Gibco), overnight at 4°C. Plates were washed with PBS, and the membrane blocked with PBS containing 5% bovine serum albumin (BSA) for 1 hour at RT. PBMCs treated with engineered T cells or control T cells were added at 5x10⁴ or 5x10³ live cells/well and incubated for 16-20 hours at 37°C, 5% CO₂. Plates were washed to remove cells and membranes incubated with anti-human IgG 550 (MT78/145, MabTech, 3850-5R) in PBS 0.1% BSA for 2 hours at RT. Fluorescence enhancement solution (MabTech, 3641-F10-60) was then added to wells. After final washes in PBS pH 7.4 (Gibco), membranes were air dried and stored in the dark. Fluorescent spots corresponding to total IgG and 9G4id IgG ASCs were quantified using an ImmunoSpot Analyzers (CTL ImmunoSpot S6 Universal M2 Analyzer, S6UNV2) at excitation 550 nm/ emission 600 nm.

Cytokine assays

Cytokines were quantified in cell culture supernatants using an IFN- γ ELISA (R&D Systems) or U-PLEX 10-plex cytokine assay for human IL-2, IL-4, IL-6, IL-8, IFN- γ , IL2R α , granzyme A, granzyme B, TNF- α , TNF- β , GM-CSF (Meso Scale Diagnostics, MSD, K151AEL-1). Samples, standards, or controls were added at 50 µL/well (MSD) or 100 µL/well (Human IFN- γ ELISA) and plates incubated for 2 hours at RT, 120 rpm. Plates were washed three times using PBS pH=7.5 0.05% Tween 20. Pre-diluted secondary antibody was added at 50 µL/well (MSD) or 100 µL/well (Human IFN- γ ELISA), and plates incubated for 1 hour at RT, 120 rpm. Following final washes, MSD Read Buffer was added at 150 µL/well and plates read using a Sector Imager 2400 (MSD). Raw electrochemiluminescence data were analyzed using the Discovery Workbench 3.0 software (MSD). A 4-parameter logistic (4PL) curve fit was generated for each analyte using standard data points to determine the concentrations of unknown samples.

BCR repertoire sequencing and analysis

For BCR repertoire analysis, cells from co-culture experiments were washed in PBS, pelleted, and stored at -80°C in Buffer RLT (Qiagen, 79216). mRNA was extracted using RNeasy RNA Extraction kits (Qiagen). Samples were amplified using BCR heavy chain (IGH) primers, and adaptome amplification was performed using iR-RepSeq+ (iRepertoire, Inc.). Next-generation sequencing libraries were generated for

each sample. Unique molecular identifiers (UMIs) were incorporated during the reverse transcription step to distinguish individual RNA molecules. Reverse transcription was performed using OneStep RT-PCR mix (Qiagen) with C-gene primer mix, followed by selection of first-strand cDNA selection and removal of remnant primers via SPRIselect bead purification (Beckman Coulter). A second round of amplification was conducted using a V-gene primer mix, followed by SPRIselect bead purification. Library amplification was performed with primers targeting communal sites engineered onto the 5' ends of the C- and V-primers. The final libraries contain Illumina dual-index sequencing adapters, a 10-nucleotide random region, and an 8nucleotide internal barcode associated with the C-gene primer. Sequencing coverage includes from within the framework 1 region to the C-region, inclusive of CDR1, CDR2, and CDR3. BCR amplified libraries were multiplexed, pooled, and sequenced on 20% of a Nextseq 1000 P1 600 cycle. RepSeq+ sequencing raw data were analyzed using iRmap. Briefly, sequence reads were de-multiplexed according to Illumina dual indices and barcode sequences. Merged reads were mapped to germline V, D, J, and C reference sequences using an IMGT reference library. CDR3 regions were identified, extracted, and translated into amino acids. The dataset was condensed by collapsing UMIs and CDR3 sequences to correct for sequencing and amplification errors. Reads sharing identical CDR3 and UMI combinations were condensed into a single UMI count. Repertoire analysis including diversity metrics, V(D)J usage, and clonal expansion was performed using Immunarch R package. The chord diagram was graphed using Circlize R106 package. The total number of reads and UMIs obtained are summarized in Supplementary Data Files S1-S9.

Statistical analyses

Statistical tests were applied to experimental group data as outlined in the figure legends and dataset. *P* values < 0.05 were considered significant, unless otherwise specified. Analyses were performed using GraphPad Prism v10.

Supplementary Materials

Supplementary Figures

Figure S1.	Design and characterization of different 9G4 CAR-T cells
Figure S2.	Long-term functional assessment of 9G4 synthetic immune receptor T cells in vitro
Figure S3.	Efficacy of 9G4 CAR-T cells and 9G4 cTCR-T cells against autoreactive 9G4id B cells
	in cold agglutinin disease (CAD) and B cell lymphoma
Figure S4.	Cytokine release by 9G4 CAR-T cells and 9G4 cTCR-T cells targeting Ramos B cells
Figure S5.	9G4 cTCR-T cells and 9G4 CAR-T cells eliminate 9G4id B cells from patients with SLE

Supplementary Tables

Table S1.	Patient characteristics
Table S2.	Frequency of B cells in SLE PBMCs and autologous engineered T cell properties
Table S3.	Nucleotide sequences of CRISPR guide RNA
Table S4.	Amino acid sequences of 9G4id and control BCRs

Other Supplementary Materials

Data Files S1-S9. IGHV sequencing data of SLE patient PBMCs treated with anti-9G4 or control T cells
 Dataset. Details and extended statistical analyses for Figures and Supplementary Figures
 Movie S1-S6. Live-cell imaging of anti-9G4 T cells targeting 9G4id or non-9G4 Ramos B cells

References

- 1. Hoi, A., Igel, T., Mok, C.C. & Arnaud, L. Systemic lupus erythematosus. *Lancet* **403**, 2326–2338 (2024).
- 2. Parra Sanchez, A.R., Voskuyl, A.E. & van Vollenhoven, R.F. Treat-to-target in systemic lupus erythematosus: advancing towards its implementation. *Nat Rev Rheumatol* **18**, 146–157 (2022).
- 3. Siegel, C.H. & Sammaritano, L.R. Systemic Lupus Erythematosus: A Review. *JAMA* **331**, 1480–1491 (2024).
- 4. Tan, E.M. Antinuclear antibodies: diagnostic markers for autoimmune diseases and probes for cell biology. *Adv Immunol* **44**, 93–151 (1989).
- 5. Crow, M.K. Pathogenesis of systemic lupus erythematosus: risks, mechanisms and therapeutic targets. *Ann Rheum Dis* **82**, 999–1014 (2023).
- 6. Arbuckle, M.R. et al. Development of autoantibodies before the clinical onset of systemic lupus erythematosus. *N Engl J Med* **349**, 1526–1533 (2003).
- 7. Sanz, I. & Lee, F.E. B cells as therapeutic targets in SLE. *Nat Rev Rheumatol* **6**, 326–337 (2010).
- 8. Furie, R.A. et al. B-cell depletion with obinutuzumab for the treatment of proliferative lupus nephritis: a randomised, double-blind, placebo-controlled trial. *Ann Rheum Dis* **81**, 100–107 (2022).
- 9. Merrill, J.T. et al. Efficacy and safety of rituximab in moderately-to-severely active systemic lupus erythematosus: the randomized, double-blind, phase II/III systemic lupus erythematosus evaluation of rituximab trial. *Arthritis Rheum* **62**, 222–233 (2010).
- 10. Aranow, C. et al. Efficacy and safety of sequential therapy with subcutaneous belimumab and one cycle of rituximab in patients with systemic lupus erythematosus: the phase 3, randomised, placebo-controlled BLISS-BELIEVE study. *Ann Rheum Dis* **83**, 1502–1512 (2024).
- 11. Rovin, B.H. et al. Efficacy and safety of rituximab in patients with active proliferative lupus nephritis: the Lupus Nephritis Assessment with Rituximab study. *Arthritis Rheum* **64**, 1215–1226 (2012).
- 12. Kamburova, E.G. et al. A single dose of rituximab does not deplete B cells in secondary lymphoid organs but alters phenotype and function. *Am J Transplant* **13**, 1503–1511 (2013).
- 13. Tur, C. et al. CD19-CAR T-cell therapy induces deep tissue depletion of B cells. *Ann Rheum Dis* **84**, 106–114 (2025).
- 14. Mougiakakos, D. et al. CD19-Targeted CAR T Cells in Refractory Systemic Lupus Erythematosus. *N Engl J Med* **385**, 567–569 (2021).
- 15. Mackensen, A. et al. Anti-CD19 CAR T cell therapy for refractory systemic lupus erythematosus. *Nat Med* **28**, 2124–2132 (2022).
- 16. Muller, F. et al. CD19 CAR T-Cell Therapy in Autoimmune Disease A Case Series with Follow-up. *N Engl J Med* **390**, 687–700 (2024).
- 17. Wang, W. et al. BCMA-CD19 compound CAR T cells for systemic lupus erythematosus: a phase 1 open-label clinical trial. *Ann Rheum Dis* **83**, 1304–1314 (2024).
- 18. Bucci, L. et al. Bispecific T cell engager therapy for refractory rheumatoid arthritis. *Nat Med* **30**, 1593–1601 (2024).

- 19. Alexander, T., Kronke, J., Cheng, Q., Keller, U. & Kronke, G. Teclistamab-Induced Remission in Refractory Systemic Lupus Erythematosus. *N Engl J Med* **391**, 864–866 (2024).
- 20. Rampotas, A., Richter, J., Isenberg, D. & Roddie, C. CAR-T cell therapy embarks on autoimmune disease. *Bone Marrow Transplant* **60**, 6–9 (2025).
- 21. Siegert, E. et al. Teclistamab in relapsed systemic sclerosis after autologous haematopoietic stem cell transplantation. *Ann Rheum Dis* **84**, 653–656 (2025).
- 22. Wudhikarn, K. et al. DLBCL patients treated with CD19 CART cells experience a high burden of organ toxicities but low nonrelapse mortality. *Blood Adv* **4**, 3024–3033 (2020).
- 23. Morris, E.C., Neelapu, S.S., Giavridis, T. & Sadelain, M. Cytokine release syndrome and associated neurotoxicity in cancer immunotherapy. *Nat Rev Immunol* **22**, 85–96 (2022).
- 24. Tavakolpour, S. et al. Antigen-Fc fusion therapy reduces severity of a model of pemphigus vulgaris without systemic immunosuppression. *Sci Transl Med* **17**, eadk6484 (2025).
- 25. Dong, Y. et al. Structural principles of B cell antigen receptor assembly. *Nature* **612**, 156–161 (2022).
- 26. Ellebrecht, C.T. et al. Reengineering chimeric antigen receptor T cells for targeted therapy of autoimmune disease. *Science* **353**, 179–184 (2016).
- 27. Mog, B.J. et al. Chimeric Autoantigen-T Cell Receptor (CATCR)-T Cell Therapies to Selectively Target Autoreactive B Cells. *Arthritis Rheumatol* **74** (2022).
- 28. Oh, S. et al. Precision targeting of autoantigen-specific B cells in muscle-specific tyrosine kinase myasthenia gravis with chimeric autoantibody receptor T cells. *Nat Biotechnol* **41**, 1229–1238 (2023).
- 29. Reincke, S.M. et al. Chimeric autoantibody receptor T cells deplete NMDA receptor-specific B cells. *Cell* **186**, 5084–5097 e5018 (2023).
- 30. Konig, M.F. The rise of precision cellular therapies. *Nat Rev Rheumatol* **20**, 69–70 (2024).
- 31. Yaniv, G. et al. A volcanic explosion of autoantibodies in systemic lupus erythematosus: a diversity of 180 different antibodies found in SLE patients. *Autoimmun Rev* **14**, 75–79 (2015).
- 32. Pincus, T. & Kaplan, A.P. True antibodies to DNA in systemic lupus erythematosus: activity of Fab and F(ab')2 fragments. *Nature* **227**, 394–395 (1970).
- 33. Winfield, J.B., Faiferman, I. & Koffler, D. Avidity of anti-DNA antibodies in serum and IgG glomerular eluates from patients with systemic lupus erythematosus. Association of high avidity antinative DNA antibody with glomerulonephritis. *J Clin Invest* **59**, 90–96 (1977).
- 34. Gomez-Banuelos, E. et al. Affinity maturation generates pathogenic antibodies with dual reactivity to DNase1L3 and dsDNA in systemic lupus erythematosus. *Nat Commun* **14**, 1388 (2023).
- 35. Sharp, G.C. et al. Association of antibodies to ribonucleoprotein and Sm antigens with mixed connective-tissue disease, systematic lupus erythematosus and other rheumatic diseases. *N Engl J Med* **295**, 1149–1154 (1976).
- 36. Tan, E.M. & Kunkel, H.G. Characteristics of a soluble nuclear antigen precipitating with sera of patients with systemic lupus erythematosus. *J Immunol* **96**, 464–471 (1966).
- 37. Harris, E.N. et al. Anticardiolipin antibodies: detection by radioimmunoassay and association with thrombosis in systemic lupus erythematosus. *Lancet* **2**, 1211–1214 (1983).
- 38. Cappione, A.J., Pugh-Bernard, A.E., Anolik, J.H. & Sanz, I. Lupus IgG VH4.34 antibodies bind to a 220-kDa glycoform of CD45/B220 on the surface of human B lymphocytes. *J Immunol* **172**, 4298–4307 (2004).

- 39. Cappione, A., 3rd et al. Germinal center exclusion of autoreactive B cells is defective in human systemic lupus erythematosus. *J Clin Invest* **115**, 3205–3216 (2005).
- 40. Silberstein, L.E. et al. Variable region gene analysis of pathologic human autoantibodies to the related i and I red blood cell antigens. *Blood* **78**, 2372–2386 (1991).
- 41. Tipton, C.M. et al. Diversity, cellular origin and autoreactivity of antibody-secreting cell population expansions in acute systemic lupus erythematosus. *Nat Immunol* **16**, 755–765 (2015).
- 42. Richardson, C. et al. Molecular basis of 9G4 B cell autoreactivity in human systemic lupus erythematosus. *J Immunol* **191**, 4926–4939 (2013).
- 43. Isenberg, D.A. et al. Correlation of 9G4 idiotope with disease activity in patients with systemic lupus erythematosus. *Ann Rheum Dis* **57**, 566–570 (1998).
- 44. Isenberg, D., Spellerberg, M., Williams, W., Griffiths, M. & Stevenson, F. Identification of the 9G4 idiotope in systemic lupus erythematosus. *Br J Rheumatol* **32**, 876–882 (1993).
- 45. Huang, W. et al. Belimumab promotes negative selection of activated autoreactive B cells in systemic lupus erythematosus patients. *JCI Insight* **3** (2018).
- 46. Cambridge, G. et al. B cell depletion therapy in systemic lupus erythematosus: effect on autoantibody and antimicrobial antibody profiles. *Arthritis Rheum* **54**, 3612–3622 (2006).
- 47. Majzner, R.G. et al. Tuning the Antigen Density Requirement for CAR T-cell Activity. *Cancer Discov* **10**, 702–723 (2020).
- 48. Mansilla-Soto, J. et al. HLA-independent T cell receptors for targeting tumors with low antigen density. *Nat Med* **28**, 345–352 (2022).
- 49. Kehry, M. et al. The immunoglobulin mu chains of membrane-bound and secreted IgM molecules differ in their C-terminal segments. *Cell* **21**, 393–406 (1980).
- 50. Peterson, M.L. Mechanisms controlling production of membrane and secreted immunoglobulin during B cell development. *Immunol Res* **37**, 33–46 (2007).
- 51. Hsiue, E.H. et al. Targeting a neoantigen derived from a common TP53 mutation. *Science* **371** (2021).
- 52. Gascoigne, N.R., Goodnow, C.C., Dudzik, K.I., Oi, V.T. & Davis, M.M. Secretion of a chimeric T-cell receptor-immunoglobulin protein. *Proc Natl Acad Sci U S A* **84**, 2936–2940 (1987).
- 53. Liu, Y. et al. Chimeric STAR receptors using TCR machinery mediate robust responses against solid tumors. *Sci Transl Med* **13** (2021).
- 54. Mog, B.J. et al. Preclinical studies show that Co-STARs combine the advantages of chimeric antigen and T cell receptors for the treatment of tumors with low antigen densities. *Sci Transl Med* **16**, eadg7123 (2024).
- 55. Roth, T.L. et al. Reprogramming human T cell function and specificity with non-viral genome targeting. *Nature* **559**, 405–409 (2018).
- 56. Dong, D. et al. Structural basis of assembly of the human T cell receptor-CD3 complex. *Nature* **573**, 546–552 (2019).
- 57. Moffett, H.F. et al. B cells engineered to express pathogen-specific antibodies protect against infection. *Sci Immunol* **4** (2019).
- 58. Dacie, J.V., Crookston, J.H. & Christenson, W.N. Incomplete cold antibodies role of complement in sensitization to antiglobulin serum by potentially haemolytic antibodies. *Br J Haematol* **3**, 77–87 (1957).

- 59. Wasastjerna, C., Dameshek, W. & Komninos, Z.D. Direct observations of intravascular agglutination of red cells in acquired autoimmune hemolytic anemia. *J Lab Clin Med* **43**, 98–106 (1954).
- 60. Potter, K.N. et al. Molecular characterization of a cross-reactive idiotope on human immunoglobulins utilizing the VH4-21 gene segment. *J Exp Med* **178**, 1419–1428 (1993).
- 61. Jefferies, L.C., Carchidi, C.M. & Silberstein, L.E. Naturally occurring anti-i/I cold agglutinins may be encoded by different VH3 genes as well as the VH4.21 gene segment. *J Clin Invest* **92**, 2821–2833 (1993).
- 62. Willims, R.C., Jr., Kunkel, H.G. & Capra, J.D. Antigenic specificities related to the cold agglutinin activity of gamma M globulins. *Science* **161**, 379–381 (1968).
- 63. Li, Y., Spellerberg, M.B., Stevenson, F.K., Capra, J.D. & Potter, K.N. The I binding specificity of human VH 4-34 (VH 4-21) encoded antibodies is determined by both VH framework region 1 and complementarity determining region 3. *J Mol Biol* **256**, 577–589 (1996).
- 64. Potter, K.N., Hobby, P., Klijn, S., Stevenson, F.K. & Sutton, B.J. Evidence for involvement of a hydrophobic patch in framework region 1 of human V4-34-encoded Igs in recognition of the red blood cell I antigen. *J Immunol* **169**, 3777–3782 (2002).
- 65. Pearlman, A.H. et al. Detection of human brain cancers using genomic and immune cell characterization of cerebrospinal fluid through CSF-BAM. *Cancer Discov* (2025).
- 66. Bikos, V. et al. Over 30% of patients with splenic marginal zone lymphoma express the same immunoglobulin heavy variable gene: ontogenetic implications. *Leukemia* **26**, 1638–1646 (2012).
- 67. Montesinos-Rongen, M., Purschke, F., Kuppers, R. & Deckert, M. Immunoglobulin repertoire of primary lymphomas of the central nervous system. *J Neuropathol Exp Neurol* **73**, 1116–1125 (2014).
- 68. Young, R.M. et al. Survival of human lymphoma cells requires B-cell receptor engagement by self-antigens. *Proc Natl Acad Sci U S A* **112**, 13447–13454 (2015).
- 69. Grande, B.M. et al. Genome-wide discovery of somatic coding and noncoding mutations in pediatric endemic and sporadic Burkitt lymphoma. *Blood* **133**, 1313–1324 (2019).
- 70. Belhouachi, N. et al. Primary vitreoretinal lymphomas display a remarkably restricted immunoglobulin gene repertoire. *Blood Adv* **4**, 1357–1366 (2020).
- 71. (!!! INVALID CITATION !!! 70).
- 72. Teachey, D.T. et al. Identification of Predictive Biomarkers for Cytokine Release Syndrome after Chimeric Antigen Receptor T-cell Therapy for Acute Lymphoblastic Leukemia. *Cancer Discov* **6**, 664–679 (2016).
- 73. Brudno, J.N. & Kochenderfer, J.N. Toxicities of chimeric antigen receptor T cells: recognition and management. *Blood* **127**, 3321–3330 (2016).
- 74. Canelo-Vilaseca, M. et al. Lymphodepletion chemotherapy in chimeric antigen receptor-engineered T (CAR-T) cell therapy in lymphoma. *Bone Marrow Transplant* **60**, 559–567 (2025).
- 75. Greco, R. et al. Innovative cellular therapies for autoimmune diseases: expert-based position statement and clinical practice recommendations from the EBMT practice harmonization and guidelines committee. *EClinicalMedicine* **69**, 102476 (2024).
- 76. Agarwal, S. et al. In Vivo Generation of CAR T Cells Selectively in Human CD4(+) Lymphocytes. *Mol Ther* **28**, 1783–1794 (2020).

- 77. Parayath, N.N., Stephan, S.B., Koehne, A.L., Nelson, P.S. & Stephan, M.T. In vitro-transcribed antigen receptor mRNA nanocarriers for transient expression in circulating T cells in vivo. *Nat Commun* **11**, 6080 (2020).
- 78. Hunter, T.L. et al. In vivo CAR T cell generation to treat cancer and autoimmune disease. *Science* **388**, 1311–1317 (2025).
- 79. Wang, Q. et al. In Vivo CD19 CAR T-Cell Therapy for Refractory Systemic Lupus Erythematosus. *N Engl J Med* (2025).
- 80. Perica, K. et al. CD4+ T-Cell Lymphoma Harboring a Chimeric Antigen Receptor Integration in TP53. *N Engl J Med* **392**, 577–583 (2025).
- 81. Ghilardi, G. et al. T cell lymphoma and secondary primary malignancy risk after commercial CAR T cell therapy. *Nat Med* **30**, 984–989 (2024).
- 82. Mok, C.C., Lau, C.S. & Wong, R.W. Risk factors for ovarian failure in patients with systemic lupus erythematosus receiving cyclophosphamide therapy. *Arthritis Rheum* **41**, 831–837 (1998).
- 83. Cervera, R. et al. Morbidity and mortality in systemic lupus erythematosus during a 10-year period: a comparison of early and late manifestations in a cohort of 1,000 patients. *Medicine* (*Baltimore*) **82**, 299–308 (2003).
- 84. Nunez, D. et al. Cytokine and reactivity profiles in SLE patients following anti-CD19 CART therapy. *Mol Ther Methods Clin Dev* **31**, 101104 (2023).
- 85. Fischbach, F. et al. CD19-targeted chimeric antigen receptor T cell therapy in two patients with multiple sclerosis. *Med* **5**, 550–558 e552 (2024).
- 86. Muller, F. et al. CD19-targeted CAR T cells in refractory antisynthetase syndrome. *Lancet* **401**, 815–818 (2023).
- 87. Morand, E. et al. Clinical, Cellular Kinetics, Pharmacodynamics and Biomarker Data Up to 12 Months After YTB323 (Rapcabtagene Autoleucel), a Rapidly Manufactured CD19 CAR-T Therapy, From an Open-Label, Phase 1/2 Study in Severe Refractory SLE. *Annals of the Rheumatic Diseases* 84, 68 70 (2025).
- 88. Sheikh, S. et al. RESET-SLE: CLINICAL TRIAL EVALUATING RESE-CEL (RESECABTAGENE AUTOLEUCEL), A FULLY HUMAN, AUTOLOGOUS 4-1BB ANTI-CD19 CAR T CELL THERAPY IN NON-RENAL SLE AND LUPUS NEPHRITIS. *Annals of the Rheumatic Diseases* **84**, 168 (2025).
- 89. Collet, A. et al. Autoreactive B cells in autoimmune diseases: Mechanisms, functions and clinical implications. *Autoimmun Rev* **24**, 103851 (2025).
- 90. Berti, A. et al. Autoreactive Plasmablasts After B Cell Depletion With Rituximab and Relapses in Antineutrophil Cytoplasmic Antibody-Associated Vasculitis. *Arthritis Rheumatol* **75**, 736–747 (2023).
- 91. Tousley, A.M. et al. Co-opting signalling molecules enables logic-gated control of CAR T cells. *Nature* **615**, 507–516 (2023).
- 92. Enbar, T. & Tang, L. Mimicking the TCR immune synapse for improved CAR-T cell function. *Cell Res* **35**, 549–550 (2025).
- 93. Xu, X. et al. Phase separation of chimeric antigen receptor promotes immunological synapse maturation and persistent cytotoxicity. *Immunity* **57**, 2755–2771 e2758 (2024).
- 94. Labanieh, L. & Mackall, C.L. CAR immune cells: design principles, resistance and the next generation. *Nature* **614**, 635–648 (2023).

- 95. Davenport, A.J. et al. Chimeric antigen receptor T cells form nonclassical and potent immune synapses driving rapid cytotoxicity. *Proc Natl Acad Sci U S A* **115**, E2068–E2076 (2018).
- 96. Friedmann-Morvinski, D., Bendavid, A., Waks, T., Schindler, D. & Eshhar, Z. Redirected primary T cells harboring a chimeric receptor require costimulation for their antigen-specific activation. *Blood* **105**, 3087–3093 (2005).
- 97. Kuwana, Y. et al. Expression of chimeric receptor composed of immunoglobulin-derived V regions and T-cell receptor-derived C regions. *Biochem Biophys Res Commun* **149**, 960–968 (1987).
- 98. Perez, R.K. et al. Single-cell RNA-seq reveals cell type-specific molecular and genetic associations to lupus. *Science* **376**, eabf1970 (2022).
- 99. Fava, A. & Rao, D.A. Cellular and molecular heterogeneity in systemic lupus erythematosus. *Semin Immunol* **58**, 101653 (2021).
- 100. Ota, M. et al. Multimodal repertoire analysis unveils B cell biology in immune-mediated diseases. *Ann Rheum Dis* **82**, 1455–1463 (2023).
- 101. Berentsen, S. et al. Cold agglutinin disease revisited: a multinational, observational study of 232 patients. *Blood* **136**, 480–488 (2020).
- 102. Cambridge, G. et al. Expression of the inherently autoreactive idiotope 9G4 on autoantibodies to citrullinated peptides and on rheumatoid factors in patients with early and established rheumatoid arthritis. *PLoS One* **9**, e107513 (2014).
- 103. Leoni, J., Ghiso, J., Goni, F. & Frangione, B. The primary structure of the Fab fragment of protein KAU, a monoclonal immunoglobulin M cold agglutinin. *J Biol Chem* **266**, 2836–2842 (1991).
- 104. Pascual, V. et al. Nucleotide sequence analysis of the V regions of two IgM cold agglutinins. Evidence that the VH4-21 gene segment is responsible for the major cross-reactive idiotype. *J Immunol* **146**, 4385–4391 (1991).
- 105. Cauerhff, A. et al. Three-dimensional structure of the Fab from a human IgM cold agglutinin. *J Immunol* **165**, 6422–6428 (2000).
- 106. Gu, Z., Gu, L., Eils, R., Schlesner, M. & Brors, B. circlize Implements and enhances circular visualization in R. *Bioinformatics* **30**, 2811–2812 (2014).

Author contributions

J.L. and M.F.K. conceived and designed the research studies; J.L., Y.X., B.J.M., C.G., E.S., D.F., B.M., T.O.A., S.G., K.J.K, T.S.A., and M.F.K. conducted experiments; R.B. and I.S. cloned SLE patient antibodies (clones 627A11, 75G12, 88F7). J.L., Y.X., and M.F.K. acquired and analyzed data; S.R.D., X.L., N.M., A.H.P., C.B., S.P., K.W.K, S.Z., F.A., and B.V. assisted with analysis and interpretation of results. J.L. and M.F.K. wrote the original draft of the manuscript; all other authors reviewed, edited, and approved the manuscript.

Acknowledgments

We thank Armaan Bahl (Johns Hopkins), Kennedy Cleage (Johns Hopkins), Ali Dbouk (Johns Hopkins), Jacqueline Douglass (Johns Hopkins), Jiaxin Ge (Johns Hopkins), Tushar Nichakawade (Johns Hopkins), Abigail McGahan (Johns Hopkins), Nickolas Papadopoulos (Johns Hopkins), and Drew Pardoll (Johns Hopkins) for their scientific and technical support. We thank Scott A. Jenks (Emory University) for his contributions cloning SLE patient antibodies. We thank Freda Stevenson for her expertise and scientific support. We thank our patients for contributing blood samples to the biorepository at Johns Hopkins. This work was supported by the National Institutes of Health (NIH) Grant R21 Al176764 (M.F.K., F.A.) and the Sol Goldman MS Research Program (M.F.K.). M.F.K. was further supported by the Lupus Research Alliance Lupus Innovation Award, the Rheumatology Research Foundation Investigator Award, the Harrington Discovery Institute Harrington Scholar-Innovator Grant, the Bisciotti Foundation Translational Fund, the Mark Fishman Foundation, the Center for Innovative Medicine Next Generation Scholar Award, the Jerome L. Greene Foundation Scholar and Discovery Awards, the Cupid Foundation, the Johns Hopkins Catalyst Award, the Peter and Carmen Lucia Buck Foundation, in addition to research support from Blackbird Laboratories, TBD Pharmaceuticals, Inc., and NorthStar Medical Radioisotopes. I.S. was supported by the Lupus Research Alliance Lupus ("Mechanistic studies of CART cell-induced B cell depletion in SLE"). C.B. was supported by NIH NCI Grant R37 CA230400. S.P. was supported by NIH NCI Grant K08 CA270403, Blood Cancer United, the American Society of Hematology Scholar award, and the Swim Across America Translational Cancer Research Award. D.W. was supported by NIH NCI Grant UG3 CA275681, U54 CA268083, and R01 CA300052. F.A. was further supported by NIH Grant R21 Al183329. C.G. was supported by NIH NHLBI Grant 5T32 HL007534. B.J.M., S.R.D., A.H.P. were supported by NIH Grant T32 GM136577. This work was further supported by The Virginia and D.K. Ludwig Fund for Cancer Research, Lustgarten Foundation for Pancreatic Cancer Research, the Commonwealth Fund, the Bloomberg-Kimmel Institute for Cancer Immunotherapy, and Bloomberg Philanthropies. The funders had no role in study design, data collection and analysis, decision to publish or preparation of the manuscript.

Data and materials availability: All data are available in the main text or the supplementary materials.